The cellular prion protein PrP^c is a partner of the Wnt pathway in intestinal epithelial cells

Laura S. Besnier[a,b,c], Philippe Cardot[a,b,c], Barbara Da Rocha[a,b,c], Anthony Simon[d,e], Damarys Loew[f], Christophe Klein[a,b,c], Béatrice Riveau[a,b,c], Michel Lacasa[a,b,c], Caroline Clair[a,b,c,*], Monique Rousset[a,b,c], and Sophie Thenet[a,b,c,g]

[a]Sorbonne Universités, Université Pierre et Marie Curie, Université Paris 06, UMRS 1138, Centre de Recherche des Cordeliers, F-75006 Paris, France; [b]Institut National de la Santé et de la Recherche Médicale, UMRS 1138, Centre de Recherche des Cordeliers, F-75006 Paris, France; [c]Université Paris Descartes, Sorbonne Paris Cité, UMRS 1138, Centre de Recherche des Cordeliers, F-75006 Paris, France; [d]Institut Curie, PSL Research University, Centre de Recherche, F-75005 Paris, France; [e]Centre National de la Recherche Scientifique/UMR144, F-75005 Paris, France; [f]Laboratoire de Spectrométrie de Masse Protéomique, Institut Curie, F-75248 Paris, France; [g]Ecole Pratique des Hautes Etudes, PSL Research University, Laboratoire de Pharmacologie Cellulaire et Moléculaire, F-75006 Paris, France

ABSTRACT **We reported previously that the cellular prion protein (PrP^c) is a component of desmosomes and contributes to the intestinal barrier function. We demonstrated also the presence of PrP^c in the nucleus of proliferating intestinal epithelial cells. Here we sought to decipher the function of this nuclear pool. In human intestinal cancer cells Caco-2/TC7 and SW480 and normal crypt-like HIEC-6 cells, PrP^c interacts, in cytoplasm and nucleus, with γ-catenin, one of its desmosomal partners, and with β-catenin and TCF7L2, effectors of the canonical Wnt pathway. PrP^c up-regulates the transcriptional activity of the β-catenin/TCF7L2 complex, whereas γ-catenin down-regulates it. Silencing of PrP^c results in the modulation of several Wnt target gene expressions in human cells, with different effects depending on their Wnt signaling status, and in mouse intestinal crypt cells in vivo. PrP^c also interacts with the Hippo pathway effector YAP, suggesting that it may contribute to the regulation of gene transcription beyond the β-catenin/TCF7L2 complex. Finally, we demonstrate that PrP^c is required for proper formation of intestinal organoids, indicating that it contributes to proliferation and survival of intestinal progenitors. In conclusion, PrP^c must be considered as a new modulator of the Wnt signaling pathway in proliferating intestinal epithelial cells.**

Monitoring Editor
Asma Nusrat
Emory University

Received: Nov 17, 2014
Revised: Jul 6, 2015
Accepted: Jul 21, 2015

INTRODUCTION

The cellular prion protein (PrP^c) has been studied essentially for its ability to undergo structural conversion into a pathogenic conformer, which is a key process for the onset of transmissible spongiform encephalopathies (Prusiner, 1998). Besides this role in prion diseases, PrP^c is expressed in a wide range of tissues and cell types, where it has been shown to contribute to the regulation of many basic biological processes, including cell proliferation, differentiation, survival, and adhesion (Westergard *et al.*, 2007). It participates in several specific functions in specialized tissues, such as neuroprotection, synaptic activity, olfaction, immune response, and epithelial and endothelial barrier function (Linden *et al.*, 2008; Petit *et al.*, 2013). PrP^c was found to be secreted mostly as a glycosylphosphatidyl inositol–anchored glycoprotein associated with lipid raft microdomains of the plasma membrane (Vey *et al.*, 1996; Naslavsky *et al.*, 1997), where it combines with several protein partners, including signaling molecules (Mouillet-Richard *et al.*, 2000; Morel *et al.*, 2004; Santuccione *et al.*, 2005). The ability of PrP^c to modulate cell signaling was proposed to mediate at least some of its biological effects (for reviews, see Westergard *et al.*, 2007; Linden *et al.*, 2008). However, the complete repertoire of PrP^c biological functions has not been determined, and analyses of different subcellular localizations

This article was published online ahead of print in MBoC in Press (http://www.molbiolcell.org/cgi/doi/10.1091/mbc.E14-11-1534) on July 29, 2015.

*In memoriam.

Address correspondence to: Sophie Thenet (sophie.thenet@crc.jussieu.fr).

Abbreviations used: PLA, proximity ligation assay; PrP^c, cellular prion protein; TCF/LEF, T-cell factor/lymphoid enhancer factor; TCF7L2, transcription factor 7–like 2; YAP, Yes-associated protein.

of the protein, as well as the identification of its site-specific partners, are important for this goal.

Among the various extraneuronal tissues that express PrP^c, previous studies from our group focused on intestine, the first site for infectious agent entry into the organism. In enterocytes, which represent the most abundant population of intestinal epithelial cells, we demonstrated that PrP^c is addressed to cell–cell junctions (Morel *et al.*, 2004), where it interacts with several desmosomal proteins (desmoglein-2, desmoplakin, γ-catenin [plakoglobin], and plakophilin-2) and participates in the structure of desmosomes (Morel *et al.*, 2008). We showed that PrP^c is required for the proper organization of adherens and tight junctions as well, thereby contributing to the intestinal barrier function (Petit *et al.*, 2012). We reported also a shortening of intestinal villi in PrP-knockout mice (Morel *et al.*, 2008), suggesting involvement of PrP^c in intestinal epithelium homeostasis.

The intestinal epithelium undergoes rapid renewal throughout life (Stappenbeck *et al.*, 1998), which requires continuous coordination between proliferation, differentiation, and death programs. Stem cells and dividing transit-amplifying cells migrate from the crypt to the villus, where most of the differentiated cells are located. In proliferating intestinal epithelial cells, that is, in the intestinal crypts in vivo or in dividing human Caco-2/TC7 enterocytes in culture, we demonstrated that a PrP^c pool was unexpectedly localized in the nucleus (Morel *et al.*, 2008). A nuclear localization of the prion protein was reported also in neuronal cells for both the protease-resistant PrP form in prion-infected cells (Mange *et al.*, 2004) and the normal PrP^c in noninfected cells (Hosokawa *et al.*, 2008). A nuclear localization signal (NLS) was described in the N-terminal domain of the mature PrP. However, this sequence was not efficient in targeting green fluorescent protein toward the nuclear compartment (Jaegly *et al.*, 1998), and the neurotoxic truncated 23-230 PrP was shown to be addressed to the nucleus independently of its NLSs (Crozet *et al.*, 2006). Although the mechanisms leading to the nuclear targeting of normal or pathological prion proteins are unknown, PrP^c was found to be associated with the lectin CBP70 in the nucleus of the NB4 human promyelocytic leukemia cell line (Rybner *et al.*, 2002) and with chromatin (Mange *et al.*, 2004), histone H3, H1-0, and lamin B1 in neuronal and β cells of the endocrine pancreas (Strom *et al.*, 2011). The latter findings suggested a role of PrP^c in transcriptional regulation, but PrP^c function in the nucleus needs to be deciphered.

To attain this objective, we first characterized the nuclear partners of PrP^c through a proteomic approach and identified γ-catenin, a component of desmosomes in differentiated cells, as a nuclear PrP^c partner in proliferating intestinal epithelial cells. γ-Catenin is a protein of the catenin family displaying a dual junctional and nuclear localization (Aktary and Pasdar, 2012). γ-Catenin is homologous to β-catenin, the core player of the canonical Wnt pathway, which drives cell proliferation in intestinal crypts and is involved in intestinal homeostasis (Pinto *et al.*, 2003; Clevers and Nusse, 2012). β-Catenin is localized at adherens junctions, where it interacts with the E-cadherin cytodomain. In the absence of Wnt stimulation, cytoplasmic β-catenin is phosphorylated by a destruction complex, which involves casein kinase 1, glycogen synthase kinase 3β, adenomatous polyposis coli, and axin, and is addressed to the proteasome for degradation. In response to Wnt activation, the destruction complex is disrupted, leading to the stabilization of the cytoplasmic β-catenin and its targeting to the nucleus, where it acts as a coactivator of the transcription factors of the T-cell factor/lymphoid enhancer factor (TCF/LEF) family to regulate the expression of many target genes involved in a variety of cellular processes (Clevers and Nusse, 2012). Although γ-catenin is known to interact with the TCF/LEF transcription factors, its exact role in the Wnt pathway is much less documented than that of β-catenin and seems to vary among different biological systems (Aktary and Pasdar, 2012).

The identification of PrP^c as a new γ-catenin nuclear partner led us to investigate whether it could interfere with the canonical Wnt pathway. Therefore, we analyzed whether PrP^c interacts with the Wnt signaling effectors β-catenin and transcription factor 7–like 2 (TCF7L2; also known previously as TCF4), the major member of the TCF family in intestine, and studied how PrP^c affects β-catenin/TCF7L2 transcriptional activity on the expression of Wnt target genes or on cell proliferation.

RESULTS

The nuclear PrP^c interacts with γ-catenin in proliferating Caco-2/TC7 enterocytes

As a first approach to determine the role of PrP^c when it is addressed to the nucleus, we undertook a proteomic analysis after immunoprecipitation of PrP^c from nuclear extracts of exponentially growing Caco-2/TC7 cells, in which we previously demonstrated the nuclear localization of a PrP^c pool (Morel *et al.*, 2008). This analysis revealed that the partners of PrP^c in the nucleus included desmoplakin and γ-catenin (plakoglobin), identified previously as PrP^c desmosomal partners in differentiated enterocytes (Petit *et al.*, 2012), along with desmoglein 1 preproprotein, glyceraldehyde-3-phosphate dehydrogenase, squamous cell carcinoma antigen (SCCA2/SCCA1), and γ-actin (Table 1).

We further focused on the interaction between PrP^c and γ-catenin. The nuclear colocalization of PrP^c and γ-catenin was confirmed by confocal microscopy in exponentially growing

Identified protein	Accession number	*Mr*	Peptide matches	Coverage (%)
Desmoplakin I	gi 1147814	331,776	9	3.7
γ-Catenin	gi 33875446	85,651	6	9.4
Squamous cell carcinoma antigen	gi 239552	44,534	5	16.7
Actin, γ1 propeptide	gi 4501887	41,792	5	19.5
Desmoglein 1 preproprotein	gi 119703744	113,747	4	6.1
Glyceraldehyde-3-phosphate dehydrogenase	gi 31645	36,054	4	16.4
SCCA2/SCCA1 fusion protein isoform 1	gi 33317676	44,648	4	12.6

Nuclear extracts from proliferative Caco-2/TC7 cells (2 d) were immunoprecipitated with anti-PrP^c antibodies. The presence of PrP^c in the resulting material was checked by Western blot before identification of the interacting proteins by liquid chromatography-MS/MS. The number of peptide matches obtained after trypsination for each protein, as well as the accession number (National Center for Biotechnology Information) and the molecular weight (*Mr*), are reported.

TABLE 1: Proteomic analysis of nuclear PrP^c partners.

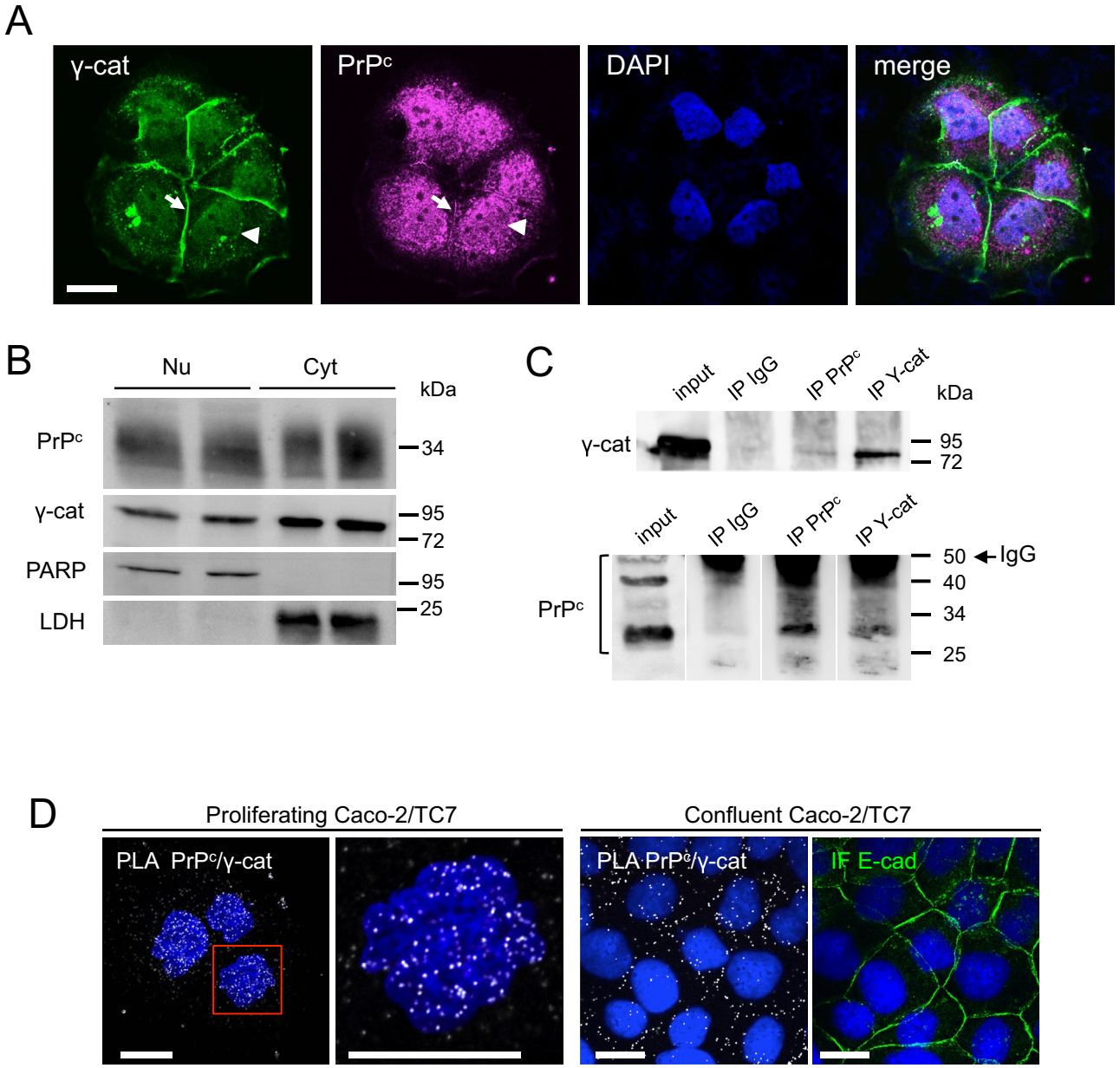

FIGURE 1: Nuclear localization of PrP^c and γ-catenin and interaction between the two proteins in proliferating Caco-2/TC7 cells. (A) Confocal analysis of exponentially growing Caco-2/TC7 cells after immunofluorescence labeling of γ-catenin (green) and PrP^c (magenta). Nuclei were stained by DAPI. Arrowheads, nuclear labeling; arrows, junctional labeling. The merge image shows that both proteins colocalize partially in the nucleus and that PrP^c is also abundant in perinuclear compartments. Bar, 20 μm. (B) Western blot analysis of nuclear (Nu) and cytoplasmic (Cyt) extracts of exponentially growing Caco-2/TC7 cells. A 30-μg amount of protein was analyzed for each fraction in duplicate. PARP and LDH were used to check the purity of nuclear and cytoplasmic fractions. (C) Nuclear extracts were immunoprecipitated with anti-PrP^c or anti–γ-catenin antibodies or with nonimmune IgG. Immunoprecipitated fractions (IP) and nuclear extracts (input) were analyzed by Western blot for γ-catenin (top) or PrP^c (bottom). Molecular weight markers are shown on the right. In the bottom, IgG is detected for IP samples even though the membrane was cut at the level of the 50-kDa marker to avoid excessive trapping of the antibody. Note that the nonglycosylated, monoglycosylated, or diglycosylated forms of PrP^c are clearly separated on this blot (whereas they may appear as a smear on other blots); a PrP^c dimer (50 kDa) is also detected in the input line. (D) PLA showing in situ interaction between PrP^c and γ-catenin (white spots) in the nucleus of proliferating Caco-2/TC7 cells (left and enlargement of the red square) and at cell–cell contacts in confluent cells. For confluent cells, immunofluorescence labeling of E-cadherin is shown in the same field. Nuclei were stained by DAPI. Bars, 10 μm.

Caco-2/TC7 cell clusters (Figure 1A). Both proteins were detected in the nucleus (arrowheads) and in the cytoplasm. Note that a portion of γ-catenin was also localized at cell–cell contacts, as was PrP^c (arrows), but with a much lower intensity, suggesting that PrP^c needs better maturation of cell–cell junctions than γ-catenin to be targeted to the membrane.

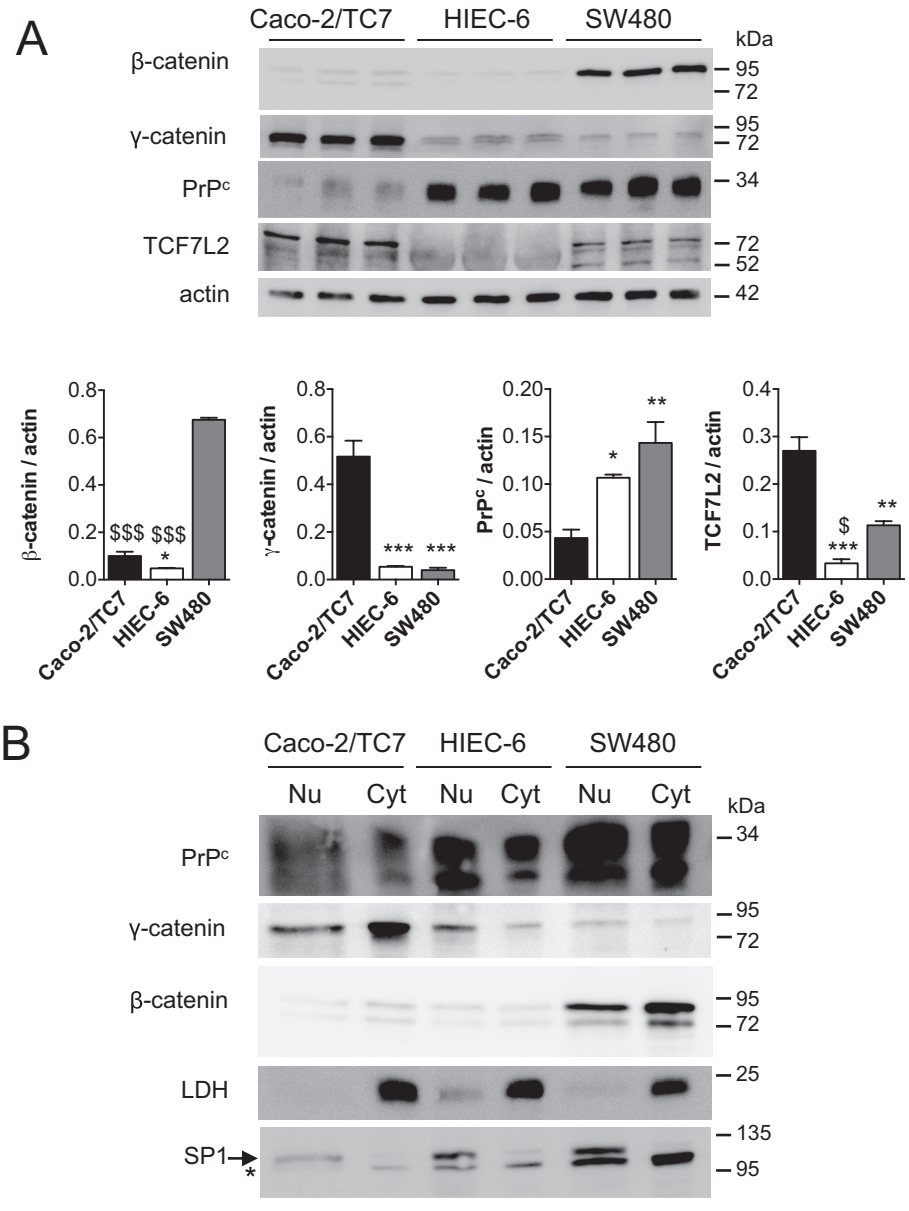

FIGURE 2: Analysis of PrP^c, γ-catenin, β-catenin, and TCF7L2 (TCF4) levels in proliferating Caco-2/TC7, HIEC-6 and SW480 cells. (A) Western blot analysis of total protein extracts from Caco-2/TC7, HIEC-6, and SW480 cells (2 d after plating). A 30-μg amount of protein was analyzed for PrP^c, γ-catenin, β-catenin, and TCF7L2 levels in each cell line in triplicate, with actin as loading control. Bar graphs show the ratio of each protein to actin after densitometric analyses (mean ± SEM; *$p < 0.05$, **$p < 0.01$ ***$p < 0.001$ vs. Caco-2/TC7; $^{\$}p < 0.05$, $^{\$\$\$}p < 0.001$ vs. SW480). (B) Western blot analysis of nuclear (Nu) and cytoplasmic (Cyt) extracts of the three cell lines. A 30-μg amount of protein was analyzed for PrP^c, γ-catenin, and β-catenin levels in each fraction and each cell line. Purity of nuclear and cytoplasmic fractions was checked by SP1 and LDH analyses; *nonspecific band revealed by the anti-SP1 antibody.

PrP^c and γ-catenin were detected in nuclear extracts by Western blot analysis (Figure 1B), and PrP^c/γ-catenin interaction was shown by coimmunoprecipitation (Figure 1C). We further confirmed that these two proteins interact in the nucleus by using in situ proximity ligation assay (PLA) and confocal microscopy (Figure 1D). This approach showed that PrP^c/γ-catenin interaction occurred mainly in the nucleus of proliferating Caco-2/TC7 cells. By contrast, this interaction was detected predominantly at cell–cell contacts in differentiated cells (Figure 1D), as observed also for the interaction between γ-catenin and another desmosomal protein, desmoplakin, as expected (unpublished data). The precision and reliability of this assay to localize interactions of endogenous proteins were assessed by the absence of PLA signal at cell–cell contacts between PrP^c and the adherens junction–associated E-cadherin, which colocalize by immunofluorescence but do not interact, as we showed previously (Morel *et al.*, 2004); in the same way, no PLA signal was detected in the nucleus between PrP^c and the transcription factor HNF-4 α (Supplemental Figure S1).

Characterization of the expression and subcellular localization of PrP^c, γ-catenin, and the Wnt effectors β-catenin and TCF7L2 (TCF4) in different intestinal cell lines

The identification of PrP^c as a new γ-catenin nuclear partner led us to investigate the possible links between this complex and the canonical Wnt pathway. We therefore analyzed the expression of PrP^c and γ-catenin, as well as that of β-catenin and TCF7L2, the major endpoint effectors of canonical Wnt signaling in intestine, during the exponential growth phase of several intestinal cell lines. With respect to their basal Wnt pathway activities, we selected three intestinal cell lines for study: the two cancer cell lines SW480, with a constitutively high activity of Wnt pathway, and Caco-2/TC7, in which Dickkopf-related protein 1 overexpression attenuates the constitutive Wnt signaling (Aguilera *et al.*, 2007), and the nontumoral crypt-like human intestinal cells HIEC-6, with a weak basal activity of Wnt pathway (Guezguez *et al.*, 2014). Consistent with Wnt pathway status, β-catenin protein level was much higher in SW480 cells than in the two other cell lines (Figure 2A). No correlation was observed between Wnt activity and PrP^c protein levels, which were similar in HIEC-6 and SW480 cells and higher than in Caco-2/TC7 cells. Of interest, the highest γ-catenin level was detected in Caco-2/TC7 cells, which have the lowest β-catenin and PrP^c levels (Figure 2A). TCF7L2 level was very low in HIEC-6 cells and twofold higher in Caco-2/TC7 than in SW480 cells. PrP^c, γ-catenin, and β-catenin were present in the nuclear fraction of the three cell lines (Figure 2B). Confocal microscopy analyses confirmed the nuclear localization of the four proteins but highlighted differences in their subcellular partitioning between the cell lines. PrP^c, γ-catenin, and β-catenin were visualized in the nucleus and the cytoplasm in both SW480 and HIEC-6 cells but with a much higher nuclear proportion in SW480 than in HIEC-6 cells (Figure 3). By contrast, even at this very low-density stage, Caco-2/TC7 cells exhibited partial junctional localization of PrP^c, γ-catenin, and β-catenin, in accordance with the well-described ability of these cells to polarize, establish mature cell–cell junctions, and differentiate (Chantret *et al.*, 1994), in

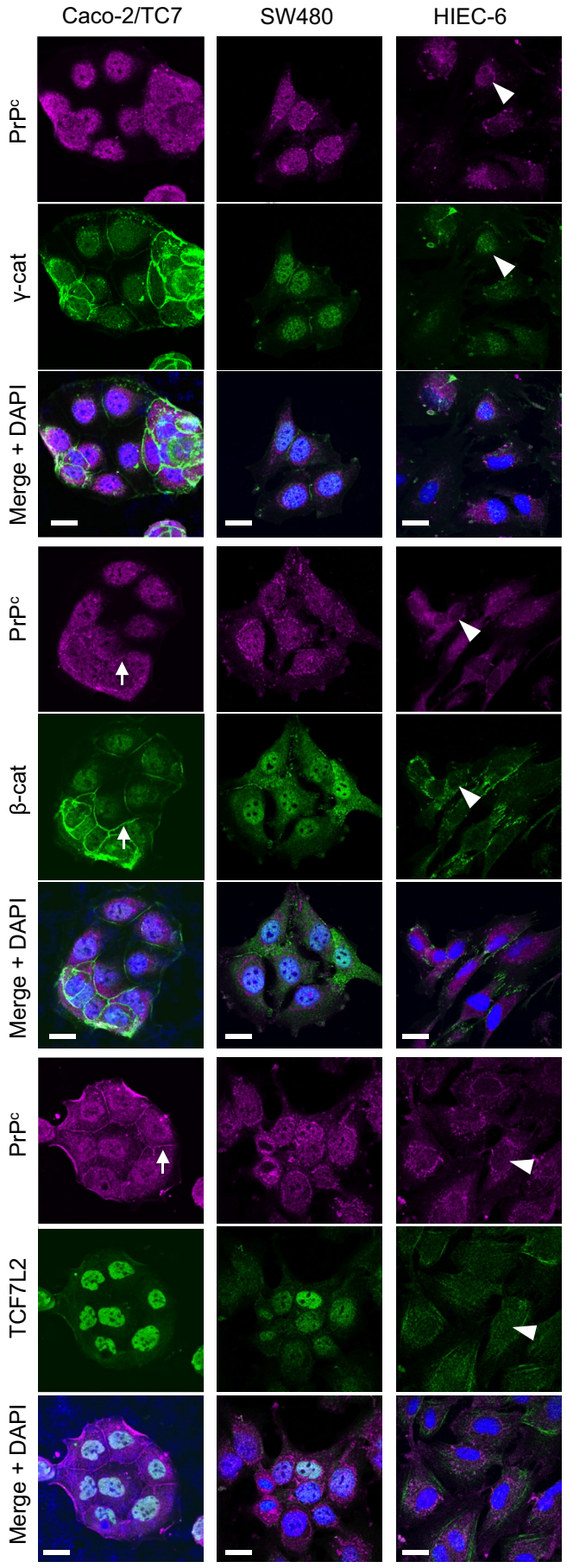

contrast to the two other cell lines. The transcription factor TCF7L2 was concentrated mostly in the nucleus in SW480 and Caco-2/TC7 cells, as expected, but was much more diffusely distributed between the cytoplasm and the nucleus in HIEC-6 cells.

PrP^c and γ-catenin interact with the Wnt effectors β-catenin and TCF7L2 in proliferating intestinal cells

γ-Catenin interacts with the transcription factor TCF7L2 (Miravet *et al.*, 2002). We hypothesized that PrP^c could thus participate in molecular complexes involving γ-catenin, β-catenin, and TCF7L2. The PLA approach was chosen to visualize protein interactions and their subcellular distribution in situ. In exponentially growing SW480, Caco-2/TC7, and HIEC-6 cells, PrP^c interacts with γ-catenin, β-catenin, and TCF7L2 (Figure 4). γ-Catenin/TCF7L2 and β-catenin/TCF7L2 interactions were detected also, as expected, and the presence of γ-catenin/β-catenin interactions confirmed the existence of multipartner complexes reported previously (Miravet *et al.*, 2002). In SW480 and Caco-2/TC7 cells, the PLA fluorescence spots were concentrated in the nucleus for all interactions, although they could be observed also in the cytoplasm. By contrast, but in agreement with the distribution of all partners as observed by immunofluorescence (Figure 3), interactions between PrP^c/γ-catenin, PrP^c/β-catenin, and γ-catenin/β-catenin occurred in much higher proportions in the cytoplasm than in the nucleus of HIEC-6 cells (Figure 4). In this cell line, complexes involving TCF7L2 were very rare, in accordance with its low level (Figures 2 and 3).

PrP^c interaction with TCF7L2 depends mostly on its β-catenin binding domain

To determine whether PrP^c interacts with TCF7L2 via β- or γ-catenin or independently of these proteins, we transfected SW480 cells with different fragments of a FLAG-TCF7L2 protein (Figure 5). Fragment expression was analyzed by immunofluorescence, and protein interactions were studied by PLA. Interactions of β-catenin, γ-catenin, and PrP^c with the full-length FLAG-TCF7L2 were easily detected in transfected cells, although the PLA signal intensity (normalized to FLAG expression) was much higher for β-catenin/FLAG-TCF7L2 interaction than for γ-catenin/FLAG-TCF7L2 or PrP^c/FLAG-TCF7L2 interactions (Figure 5A). These results are in accordance with the differences observed for interactions of each protein with the endogenous TCF7L2 (Figure 4). When FLAG-TCF7L2 constructs were deleted for the binding domains of β-catenin (del 1–51) or of both β- and γ-catenin (del 2–100), their interaction with β-catenin was completely lost (Figure 5B). This result is in agreement with the glutathione *S*-transferase pull-down approach, which was used previously to identify these binding sites (Miravet *et al.*, 2002), thus demonstrating the accuracy of the PLA technique. The deletion of the catenin-binding domains decreased interactions of TCF7L2 with PrP^c by 85 and 90% for del 1–51 and del 2–100 constructs, respectively, and with γ-catenin by 80% for both

FIGURE 3: Subcellular distribution of PrP^c, β-catenin, γ-catenin, and TCF7L2 in proliferating Caco-2/TC7, SW480, and HIEC-6 cells. Cells were immunolabeled for PrP^c and γ-catenin (top three), PrP^c and β-catenin (middle three), or PrP^c and TCF7L2 (bottom three) and analyzed by confocal microscopy. Merge images with DAPI staining are shown for each labeling. Arrowheads show the faint nuclear labeling of all proteins in HIEC-6 cells, and arrows point out junctional labeling of PrP^c, β-catenin, and γ-catenin in Caco-2/TC7 cells. Bars, 20 μm.

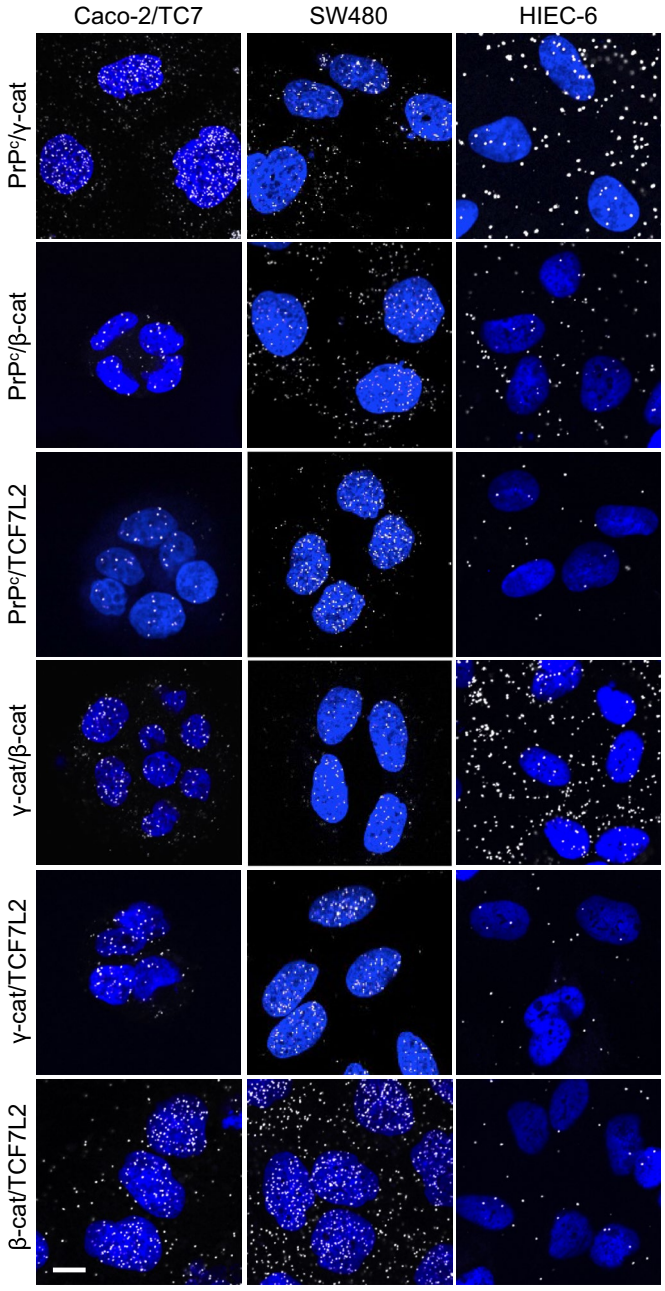

FIGURE 4: PrP^c interacts with γ-catenin and the Wnt pathway effectors β-catenin and TCF7L2 in Caco-2/TC7, SW480, and HIEC-6 cells. PLA showing in situ interaction (white spots) between PrP^c, γ-catenin, β-catenin, and TCF7L2 in proliferating cells for each cell line. PLA assays were performed between the pair of proteins indicated on the left. Nuclei were stained by DAPI. Note that interactions are detected mainly in the nucleus for Caco-2/TC7 and SW480 cells and mainly in the cytoplasm for HIEC-6 cells. Bar, 10 μm.

constructs. Interactions with β-catenin were restored partially for the construct deleted for the 52–143 fragment and totally for the construct deleted for the 82–143 fragment, as expected. Very similar results were obtained for interactions of PrP^c with these constructs. By contrast, interactions with γ-catenin remained very low with the del 52–143 construct, as expected, and were only partially restored with the del 82–143 fragment, probably because this deletion affects the conformation of the γ-catenin–binding domain.

Interactions between β-catenin or PrP^c and TCF7L2 can occur in the cytoplasm, as shown by analyses of TCF7L2 mutants obtained by serial deletions of ~100 amino acids from the C-terminal part of the protein comprising or not the NLS (Supplemental Figure S2). Interactions of TCF7L2 with both proteins were detected mostly in the nucleus with fragments 1–500 and 1–420, in the cytoplasm, and around the nucleus with the 1–307 fragment, which is devoid of NLS, but were concentrated again in the nucleus with the 1–201 fragment, which is small enough to diffuse inside this compartment (Supplemental Figure S2).

The foregoing results showed that PrP^c interaction with TCF7L2 depends mostly on the β-catenin–binding domain. To examine further whether PrP^c interacts with TCF7L2 through β-catenin, we studied the effect of β- or γ-catenin silencing by small interfering RNA (siRNA) on PrP^c/TCF7L2 interactions in both nuclear and cytoplasmic compartments. On silencing of β-catenin, which was decreased by >90% in both cytoplasm and nucleus (Figure 6A), PrP^c/TCF7L2 interactions were significantly decreased (Figure 6B). This loss of interactions affected the nucleus compartment (–25%), with no effect on cytoplasmic interactions (Figure 6B, compare hatched bars with white bars). However, this decrease of nuclear interactions was modest, most of them being maintained in the absence of β-catenin. γ-Catenin silencing (–80% for total level, –70% for nuclear level; Figure 6A) had no effect on PrP^c/TCF7L2 interactions in the cytoplasm or the nucleus (Figure 6B). Moreover, the silencing of one catenin had no significant effect on the interaction of PrP^c with the other catenin.

PrP^c up-regulates the transcriptional activity of the β-catenin/TCF7L2 complex

We then addressed the functional role of PrP^c in the Wnt signaling pathway, using a transcriptional reporter assay, and compared it to that of γ-catenin, which has been suggested to exert a negative effect on TCF7L2-mediated transcription (Miravet 2002). TOP or FOP reporter plasmids were cotransfected in COS7 cells together with a constitutively activated form of β-catenin and either PrP^c or γ-catenin. PrP^c increased the luciferase activity induced by β-catenin in a dose-dependent manner, whereas γ-catenin decreased it (Figure 7A). In SW480 cells, which have a constitutively high β-catenin level, we confirmed these opposite effects of PrP^c and γ-catenin (Figure 7B). Positive regulation of the transcriptional activity of the β-catenin/TCF7L2 complex by PrP^c was further demonstrated by decreased luciferase activity upon PrP^c silencing by siRNA and its rescue upon cotransfection with mouse PrP^c, which is not affected by the siRNA (Figure 7C; for siRNA efficiency, see Figure 8A and Supplemental Figure S3).

PrP^c knockdown affects expression of Wnt and Hippo target genes

PCR array analyses were then performed to evaluate changes in the expression of a large panel of Wnt target genes in response to PrP^c or γ-catenin silencing. Experiments were conducted on SW480 and HIEC-6 cells, which differ greatly in their Wnt pathway activity levels. Caco-2/TC7 cells were not analyzed because the presence of a desmosome-associated pool of PrP^c and γ-catenin in these cells, even at very early stages of the culture, could render the results difficult to interpret. Efficiency of silencing by siRNA was shown by a net decrease of the corresponding mRNA levels (Figure 8A). Protein levels were reduced by 70–90% in both total cell lysates and nuclear extracts of SW480 or HIEC-6 cells from 24 h after transfection (Supplemental Figure S3). This processing time was then chosen for further analyses.

Among the 84 Wnt target genes that were analyzed, the expression of 29 was modulated in at least one cell line upon either PrP^c or γ-catenin siRNA treatment (Figure 8B). Surprisingly, PrP^c silencing in SW480 cells resulted in the increased expression of 15 genes (≥1.4-fold), with no decreased gene expression (≤0.7-fold; Figure 8C). The expression of half of these 15 genes was increased also upon PrP^c silencing in HIEC-6 cells, in which basal Wnt activity is very low, but, in addition, the expression of seven genes was reduced in these cells (Figure 8C). The effect of γ-catenin silencing was similar to that of PrP^c silencing for most of the genes whose expression was modulated in HIEC-6 cells but differed markedly from that of PrP^c silencing in SW480 cells (Figure 8B). The classical transcriptional TCF7L2 targets, *MYC*, *CCND1*, and *AXIN2*, were not significantly modulated by PrP^c or γ-catenin silencing, even though the expression of the three genes tended to increase when analyzed by quantitative PCR (qPCR) in SW480 cells (Supplemental Figure S4).

To determine whether PrP^c could interfere with the expression of Wnt target genes in vivo, the mRNA level of eight genes whose expression was modulated in cell lines (Figure 8B), as well as that of *Myc* and *Ccnd1*, was analyzed in wild-type and PrP-knockout mice in the bottom of intestinal crypts, where high Wnt activity is observed in vivo (Figure 8D). The expression of seven genes was increased in crypt cells in the absence of PrP^c. They include *Myc* and *Ccnd1*, whose expression was not significantly modulated in cell lines; *Sox9*, *Ets2*, *Irs1*, and *Gja1*, whose expression was increased in SW480 cells upon PrP^c silencing; and also *Id2*, whose expression was decreased in HIEC-6 only. The expression of *Igf2*, *Fgf9*, and *Tcf4* (new nomenclature) was not modified. None of the tested genes showed a decreased expression in crypt cells of PrP-knockout as compared with wild-type mice.

The apparently conflicting data in TOP/FOP reporter assays and PCR array analyses, as well as the effect of PrP^c or γ-catenin silencing on the expression of Wnt target genes in HIEC-6 cells, in which nuclear β-catenin and TCF7L2 levels are very low, indicate that PrP^c or γ-catenin could modulate Wnt target gene expression through other transcriptional effectors. Because some of these genes are also transcriptional targets of the Yes-associated protein (YAP)/TEAD complex, an effector of the Hippo pathway (Zhao *et al*., 2008), we analyzed whether interaction between PrP^c and YAP could occur. Confirming this hypothesis, PLA analyses revealed the presence of PrP^c/YAP complexes in both the cytoplasm and nucleus of proliferating HIEC-6, Caco-2/TC7, and SW480 cells (Figure 9).

PrP^c is required for proper intestinal organoid formation

The Wnt pathway is a driving force for cell proliferation in intestinal crypts (Clevers and Nusse 2012). The up-regulation of β-catenin/TCF7L2 transcriptional activity by PrP^c prompted us to examine a possible effect of PrP^c on cell proliferation. We observed previously a transient arrest of cell proliferation after PrP^c knockdown by siRNA in Caco-2/TC7 cells (Morel *et al*., 2008). We confirmed this result in HIEC-6 cells but not in SW480 cells, in which, however, PrP^c overexpression induced a slight increase in cell proliferation (unpublished data). We considered that the possible role of PrP^c in cell proliferation could be studied more accurately in a model of normal intestinal progenitor cells. We isolated crypts from wild-type and PrP-knockout mice and performed intestinal organoid cultures (Sato *et al*., 2009). Figure 10A shows a net decrease of frequency in organoid formation from PrP^c-knockout compared with wild-type mice. The few organoids that were obtained displayed the expected organization, with regular E-cadherin and β-catenin membrane staining (Figure 10C) and accumulation of apoptotic cells in the internal lumen (unpublished data) but were in general smaller (Figure 10B) and showed less-developed crypt domains (Figure 10, B and C) than the organoids developed from the wild-type crypts.

These results could be linked to weaker Wnt activity in intestinal epithelial crypt cells from PrP^c-knockout mice. We compared β-catenin nuclear staining in the bottom of intestinal crypts from wild-type and PrP-knockout mice and observed a decreased frequency of cells exhibiting a clear nuclear localization of β-catenin in PrP-knockout crypts (Figure 11).

DISCUSSION

We identified the nuclear partners of PrP^c in proliferating intestinal epithelial cells and showed a new role for this protein in the modulation of Wnt pathway. PrP^c interacts not only with γ-catenin, one of its desmosomal partner (Morel *et al*., 2008), but also with β-catenin and TCF7L2, which are the main effectors of Wnt pathway in intestinal cells, the β-catenin–binding domain of TCF7L2 being crucial for its interaction with PrP^c. Furthermore, we demonstrate that PrP^c modulates the expression of several Wnt target genes, has a positive effect on the transcriptional activity of the β-catenin/TCF7L2 complex, and is required for establishing intestinal organoids ex vivo.

We showed the presence of a nuclear pool of PrP^c in two adenocarcinoma cell lines, SW480 and Caco-2/TC7 cells, as well as in normal crypt-like cells, HIEC-6 (Figure 2), in accordance with our previous results in human intestinal crypts (Morel *et al*., 2008). However, it should be noted that PrP^c was less concentrated in the nucleus of HIEC-6 cells, which exhibit a very low Wnt activity, than in the two other cell lines, in which the effectors of Wnt pathway are present in the nucleus (Figure 3). Because PrP^c lacks a functional NLS (Jaegly *et al*., 1998), it likely needs a partner to be imported into the nucleus. TCF7L2 could be such a partner, as was suggested for β-catenin (Shitashige *et al*., 2008). By the use of PLA, which allows visualization of the subcellular localization of protein interactions, we showed that PrP^c can interact with β-catenin, γ-catenin, and TCF7L2 outside the nucleus. This was observed for the interactions of endogenous proteins (Figure 4) and for PrP^c or β-catenin interactions with TCF7L2 constructs lacking their NLS (Supplemental Figure S2). PrP^c interactions with β-catenin, γ-catenin, and TCF7L2 were concentrated in nucleus only in the context of high Wnt activity and TCF7L2 levels, that is, in SW480 and Caco-2/TC7 cells and not in HIEC-6 cells (Figure 4). These results suggest that multipartner complexes are formed in the cytoplasm before their nuclear import via the classical NLS of TCF7L2.

Combining the use of TCFL2 mutants and β-catenin silencing (Figures 5 and 6), we showed that β-catenin mediates a portion of PrP^c/TCF7L2 interactions through the β-catenin–binding domain of TCF7L2 but that other intermediate proteins and/or a direct interaction between PrP^c and TCF7L2 may also exist. By contrast, the presence of the γ-catenin–binding domain of TCF7L2 has no influence on its interaction with PrP^c, and, accordingly, γ-catenin silencing does not modulate these interactions (Figures 5 and 6), even though PrP^c/γ-catenin and γ-catenin/TCF7L2 complexes are observed (Figures 1 and 4). Finally, our results in HIEC-6 cells suggest that PrP^c and β-catenin may interact also independently of TCF7L2 (Figure 4). Involvement of PrP^c in these multiple combinations of protein complexes, whose composition most probably differs between cytoplasm and nucleus, could modify either the nuclear import of the Wnt effectors or their activity in the nucleus.

The transcription factor complex β-catenin/TCF7L2 is responsible for the transcriptional modulation of Wnt target gene expression in intestinal epithelial cells (Hatzis *et al*., 2008). The γ-catenin/TCF7L2 complex was shown to be inefficient in binding to DNA (Zhurinsky *et al*., 2000; Miravet *et al*., 2002). It was suggested

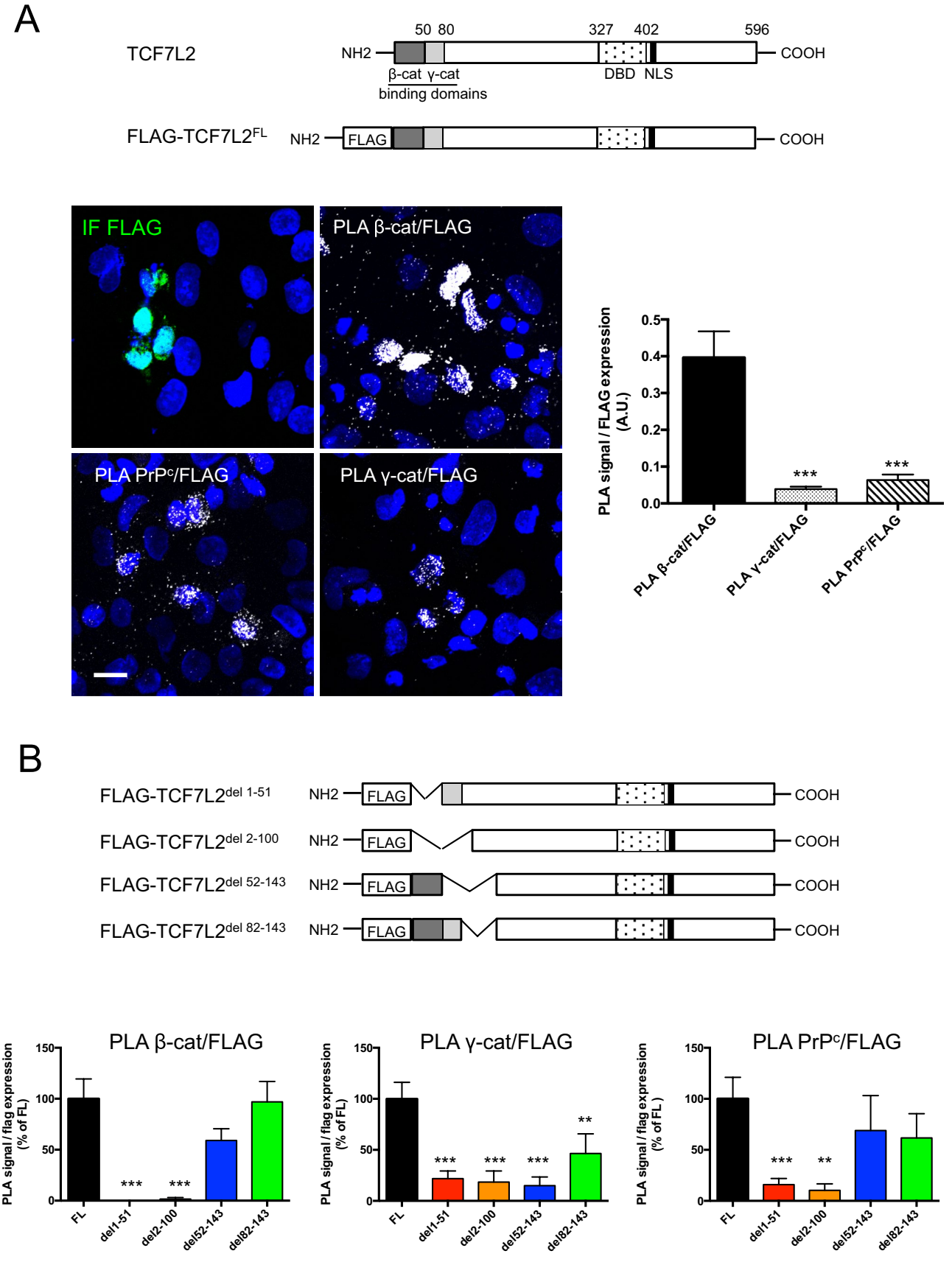

FIGURE 5: PrP^{c} interaction with the transcription factor TCF7L2 occurs mainly via the β-catenin–binding domain of TCF7L2. (A) Schematic diagram of the human TCF7L2 protein and the full-length TCF7L2 tagged with the FLAG octapeptide (FLAG-TCF7L2^{FL}) construct. SW480 cells were transfected with FLAG-TCF7L2 ^{FL}. Transfected cells were immunolabeled using an anti-FLAG antibody (IF FLAG), and PLA was performed using anti-FLAG and anti–β-catenin

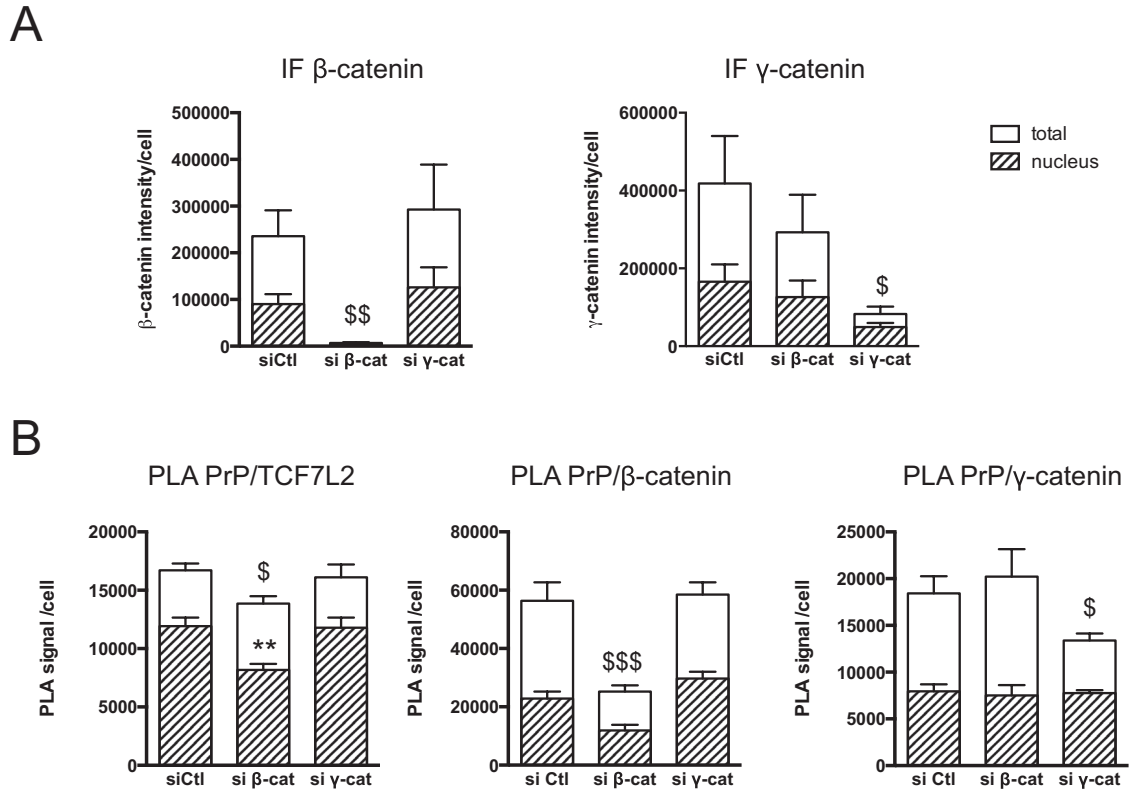

FIGURE 6: Effect of β-catenin or γ-catenin silencing on PrP^c/TCF7L2 interactions. SW480 cells were transfected with the indicated siRNAs and analyzed after 48 h. (A) Decrease of β-catenin or γ-catenin protein levels was evaluated by immunofluorescence labeling (IF). Graphs present the quantification of total (white bars) or nuclear (hatched bars) IF signal, measured in five random fields (~300 cells; mean ± SEM; $^{\$}p < 0.05$ and $^{\$\$}p < 0.01$ vs. siCtl for total signal). (B) Evaluation by PLA of the interactions of PrP^c with TCF7L2, β-catenin, or γ-catenin. Graphs present the quantification of total (white bars) or nuclear (hatched bars) PLA signal per cell measured in at least 10 random fields (~800 cells; mean ± SEM; $^{\$}p < 0.05$ and $^{\$\$\$}p < 0.001$ vs. siCtl for total PLA signal; $^{**}p < 0.01$ vs. siCtl for nuclear signal).

previously that γ-catenin exerts by itself a negative regulation of TCF7L2 transcriptional activity (Miravet *et al.*, 2002) but, through its ability to displace β-catenin from adherens junctions or from the destruction complex, can also enhance the β-catenin/TCF7L2 pool (Salomon *et al.*, 1997; Aktary and Pasdar, 2012). In the present study, we observed a negative modulation of TCF7L2 transcriptional activity by γ-catenin. By contrast, we establish for the first time a positive regulation of this activity by PrP^c (Figure 7). Because activation of the Wnt pathway is necessary for proliferation of intestinal epithelial cells, this result is in agreement with 1) the impairment of growth and survival of intestinal organoids from PrP-knockout mice (Figure 10), and 2) the alteration of nuclear β-catenin localization in intestinal crypts of PrP-knockout mice (Figure 11). This could explain the shortening of the villi that we described previously in PrP^c-knockout mice (Morel *et al.*, 2008) and is in accordance with the positive role of PrP^c in gastric cancer cell proliferation mediated by phosphoinositide 3-kinase/Akt (Liang *et al.*, 2007), a pathway that may interfere with several steps of Wnt signaling (Yan and Lackner, 2012).

In this context, the increased expression of several Wnt target genes upon PrP^c silencing seems contradictory—in particular, in crypts of PrP-knockout mice, the up-regulation of *Myc* and *Ccnd1*, which are well known to mediate effects of Wnt signaling on cell proliferation (van de Wetering *et al.*, 2002). Compensatory effects in knockout mice cannot explain these discrepancies, since the same tendency was observed in SW480 cells soon after PrP^c silencing. In HIEC-6 cells, in which nuclear β-catenin and TCF7L2 levels are very low, PrP^c and γ-catenin are able to modulate the expression of genes

(PLA β-cat/FLAG), anti–γ-catenin (PLA γ-cat/FLAG), or anti-PrP^c antibodies (PLA PrP^c/FLAG). Nuclei were stained by DAPI (bar, 20 μm). Graphs present the quantifications of PLA signal for each interaction normalized to values of IF FLAG signal, measured in at least 10 random fields (~1000 cells/experiment) in two independent experiments (A.U., arbitrary units; mean ± SEM; $^{***}p < 0.001$ vs. PLA β-cat/FLAG). NLS, nuclear localization signal; DBD, DNA-binding domain. (B) Schematic diagram of the different FLAG-TCF7L2 deletion constructs. TCF7L2 lacking the β-catenin interaction domain (TCF7L2$^{del\ 1\text{-}51}$), lacking both β- and γ-catenin interaction domains (TCF7L2$^{del\ 2\text{-}100}$), lacking the 52–82 γ-catenin interaction domain (TCF7L2$^{del\ 52\text{-}143}$), or deleted for a sequence adjacent to the γ-catenin interaction domain (TCF7L2$^{del\ 82\text{-}143}$). Experiments were conducted as in A. Graphs present the quantifications of PLA signal normalized to values of IF FLAG signal for each construct. Measurements were performed as described in A. For each interaction, results obtained with the different constructs are presented as percentage of the value obtained with the full-length (FLAG-TCF7L2^{FL}) construct (mean ± SEM; $^{**}p < 0.01$ and $^{***}p < 0.001$ vs. FL).

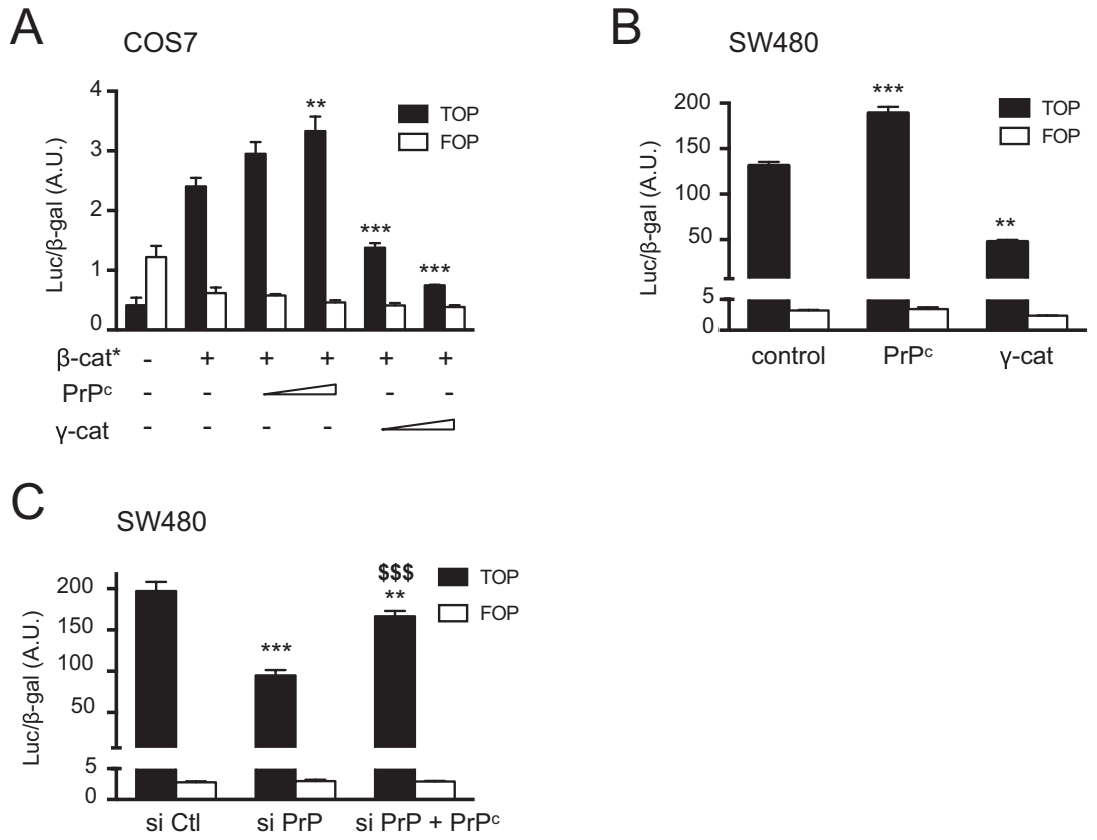

FIGURE 7: The TCF7L2/β-catenin transcriptional activity is up-regulated by PrP^c and down-regulated by γ-catenin. (A) COS7 cells were transfected with luciferase reporter plasmids containing TCF-binding sites (TOP) or mutated TCF-binding sites as negative control (FOP) and a LacZ expression plasmid as internal control. Expression vectors for constitutively active S33Y mutant of β-catenin (β-cat*), PrP^c, or γ-catenin were cotransfected as indicated. Values represent mean ± SEM of luciferase activity normalized to corresponding β-Gal activity. $^{**}p < 0.01$; $^{***}p < 0.001$ vs. β-cat* alone. (B) SW480 cells were transfected with the TOP/FOP reporters and LacZ plasmid and cotransfected with empty vector (control) or PrP^c or γ-catenin expression plasmids as indicated. $^{**}p < 0.01$, $^{***}p < 0.001$ vs. control. (C) SW480 cells were transfected with the TOP/FOP reporters and LacZ plasmid, together with a control siRNA (siCtl), PrP^c siRNAs (siPrP), or PrP^c siRNAs combined with a mouse PrP^c expression vector (siPrP+PrP^c). $^{**}p < 0.01$, $^{***}p < 0.001$ vs. siCtl; $^{\$\$\$}p < 0.001$ vs. siPrP. Experiments were all performed in triplicate, and the graphs present one experiment representative of two or three independent experiments for each condition.

identified as Wnt targets, suggesting that both proteins interfere with the activity of other transcriptional effectors as well. Multiple cross-talks between the Wnt and Hippo pathways have been shown (Azzolin *et al.*, 2012; Rosenbluh *et al.*, 2012). In this study, we showed an interaction of PrP^c with the transcriptional coactivator YAP, which is one effector of Hippo pathway (Figure 9). Thus PrP^c could be also a partner of this pathway, as shown recently for desmosomal γ-catenin in arrhythmogenic cardiomyopathy (Chen *et al.*, 2014). PrP^c interacts with YAP in both cytoplasm and nucleus, two compartments where YAP may exert opposite effects on Wnt effectors and cell proliferation (Moroishi *et al.*, 2015). Whether and how PrP^c modulates the transcriptional activity of YAP/ or TAZ/TEAD complexes remain to be explored. Nevertheless, our results argue strongly for a role of PrP^c in the regulation of gene transcription beyond the β-catenin/TCF7L2 complex and Wnt classical targets associated with cell proliferation.

During the past decade, several studies have established a positive correlation between PrP^c expression and tumor aggressiveness or adenoma-to-carcinoma progression (for review, see Antony *et al.*, 2012). Our results, which establish an interaction of PrP^c with effectors of Wnt and Hippo pathways, both clearly involved in cancer (Clevers and Nusse, 2012; Moroishi *et al.*, 2015), opens a new field of research on the mechanisms and signaling pathways that link PrP^c—not only its expression, but also its subcellular localization and the complexes in which it is involved—to colorectal cancers.

In conclusion, PrP^c is targeted toward desmosomes or nucleus in intestinal epithelial cells and shares roles with the armadillo family proteins β- and γ-catenin in cell–cell adhesion and cell signaling leading to the regulation of the Wnt pathway. We propose that nuclear PrP^c acts as a coregulator able to finely tune the final steps of Wnt signaling and potentially other related pathways involved in the regulation of intestinal epithelium homeostasis.

MATERIALS AND METHODS

Cell culture

All culture media were purchased from Life Technologies/Invitrogen (Cergy-Pontoise, France). Caco-2/TC7 cells (Chantret *et al.*, 1994) were cultured as previously described (Morel *et al.*, 2008). SW480 and COS7 cells were cultured in high-glucose DMEM GlutaMAX I supplemented with 10% heat-inactivated fetal bovine serum (Eurobio/Abcys, Les Ulis, France) and with (SW480) or without (COS7) 1%

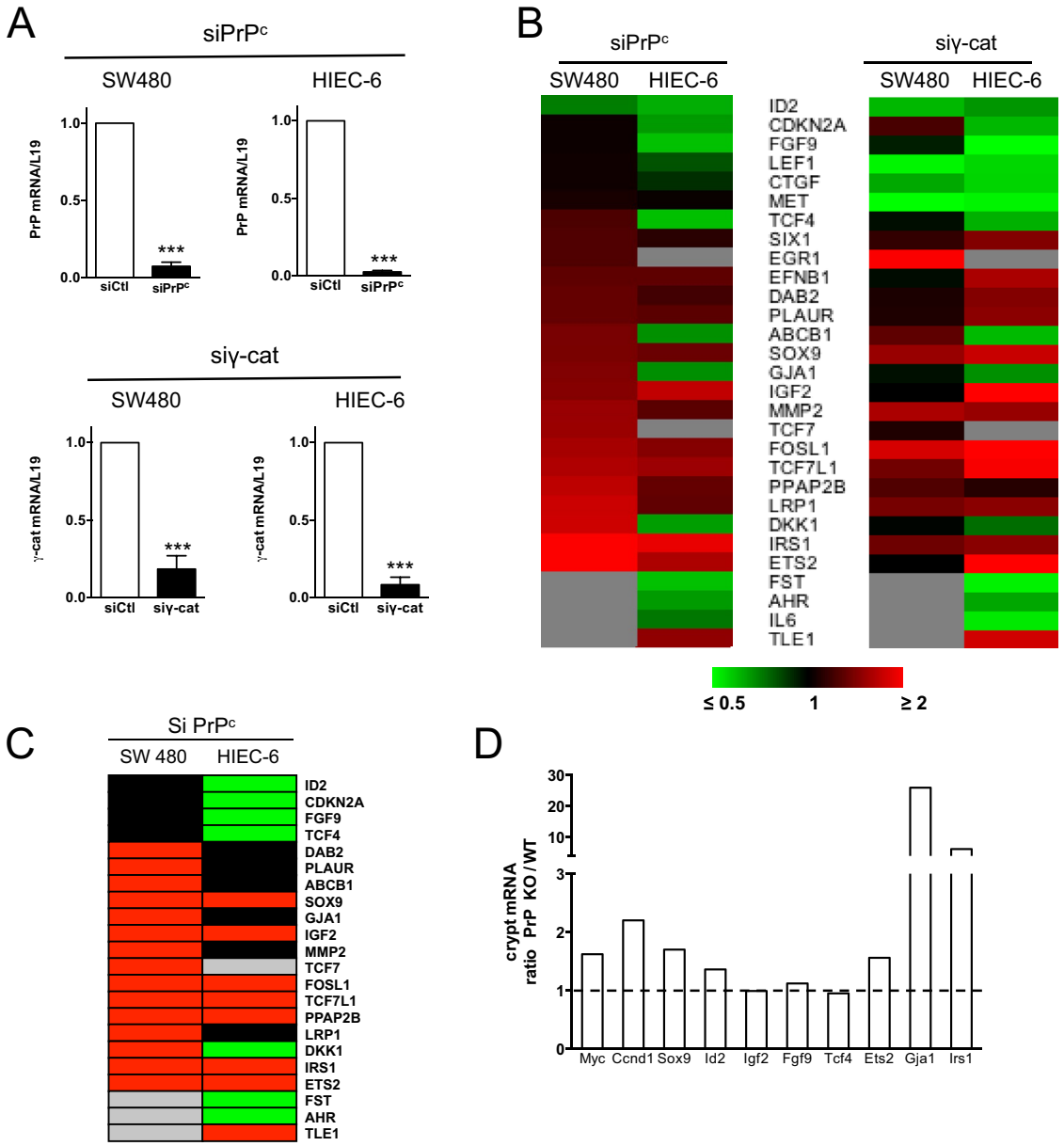

FIGURE 8: PrP^c and γ-catenin silencing modulates the expression of several Wnt target genes with different effects in SW480 and HIEC-6 cells. (A) PrP^c and γ-catenin knockdown in SW480 and HIEC-6 cells upon siRNA transfection. Decrease of PrP^c or γ-catenin mRNA at 24 h after transfection with the corresponding pairs of siRNAs. mRNA levels were determined by RT-qPCR and normalized to L19 levels. For each cell line, results are normalized to mRNA levels in cells transfected with control siRNA, which were set at 1 (mean ± SEM from three independent experiments; ***$p < 0.001$ vs. cells transfected with control siRNA). (B) Heat maps illustrating the modifications of Wnt target gene expression 24 h after PrP^c or γ-catenin siRNA transfection in each cell line (analysis of 84 Wnt target genes). Genes whose expression was modulated (≤0.7- or ≥1.4-fold) in at least one cell line by one siRNA were selected (mean of $n = 3$ independent experiments for each siRNA in each cell line; $p < 0.05$ for each gene in each cell line as compared with control siRNA). Genes were ranked according to the modulation factor of their expression in SW480 cells upon PrP^c silencing. Gray indicates undetected expressions. Note that the TCF4-modulated gene appearing in the heat map (also known as ITF2 or SEF2) differs from TCF7L2 (widely known as TCF4). (C) Pseudo heat map after selection of the genes whose expression is increased ≥1.4-fold (red) or decreased ≥0.7-fold (green) after PrP^c silencing in each cell line. Black, modulation factor between 0.7 and 1.4; gray, undetected expression. (D) Analysis of several Wnt target genes in the fraction of epithelial cells corresponding to the crypt bottom of wild-type (WT) and PrP-knockout (PrP KO) mice (pool of five mice for each genotype). mRNA levels were determined by RT-qPCR and normalized to cyclophilin levels. Results are expressed as the ratio of expression in PrP^c-knockout vs. WT mice for each gene.

nonessential amino acids. Nontumoral crypt-like human intestinal cells HIEC-6, kindly provided by J.-F. Beaulieu (Department of Anatomy and Cell Biology, University of Sherbrooke, Sherbrooke, Canada), were cultured in OPTIMEM-GlutaMAX supplemented with 5% fetal bovine serum, 10 mM 4-(2-hydroxyethyl)-1-piperazineethane-sulfonic acid (HEPES; Life Technologies/Invitrogen), and 5 ng/ml EGF

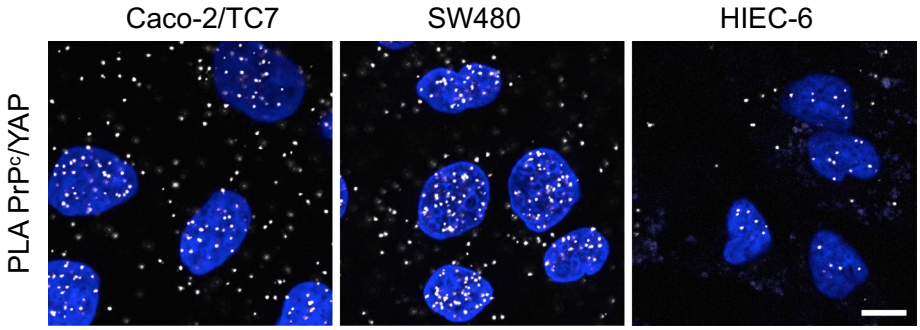

FIGURE 9: PrP^c interacts with YAP, the effector of the Hippo pathway. PLA was performed in proliferating Caco-2/TC7, SW480, and HIEC-6 cells to reveal interactions between endogenous YAP and PrP^c. Note that, although present also in the cytoplasm, interaction signals were concentrated in the nucleus, even for HIEC-6 cells. Bar, 10 μm.

(BD Biosciences, Le Pont de Claix, France). Depending on experiments, cells were plated on 3-μm–pore size microporous polyethylene terephthalate filters (Transwell; Corning, Fisher, Illkirch, France), glass coverslips (Polylabo, Strasbourg, France), or plastic (Corning, Fisher).

Mass spectrometry analysis

Proliferating Caco-2/TC7 cells were washed twice in 10 mM Tris-HCl, pH 7.5, containing 20 mM KCl, 2 mM $CaCl_2$, 2 mM $MgCl_2$, and 0.2 mM spermidine (TKCM buffer) and scraped in TKCM containing 1% Triton X-100, 1 mM phenylmethylsulfonylfluoride, antiproteases, and antiphosphatases.

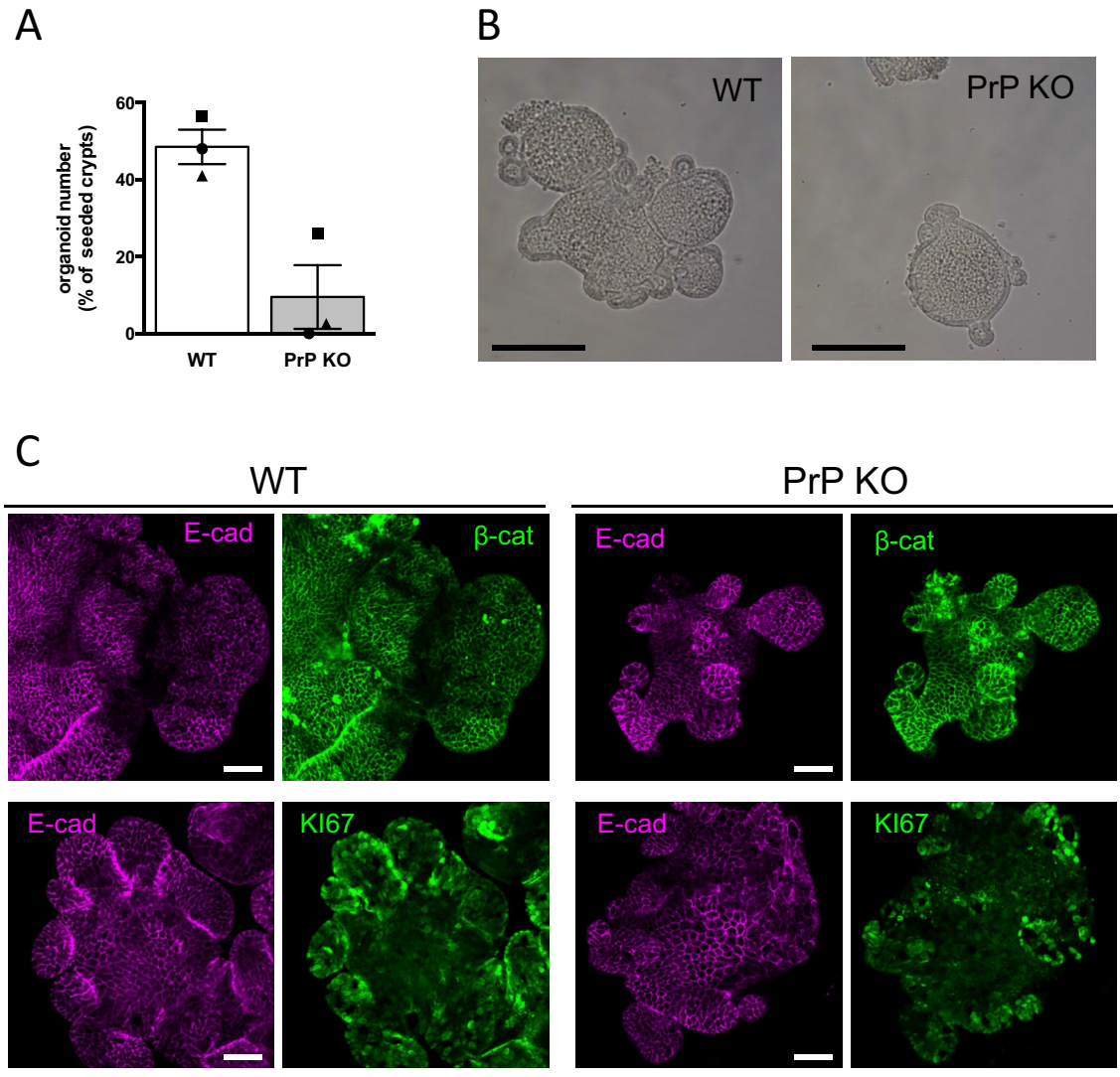

FIGURE 10: Formation of intestinal organoids is impaired in the absence of PrP^c. (A) Organoid initiation frequency from intestinal crypts of WT or PrP KO mice. The symbols represent the mean numbers of organoids per well 6 d after seeding (2–6 wells/experiment) expressed as percentage of plated crypts. Bars represent the mean ± SEM from the three independent experiments. (B) Phase contrast microscopy images 7 d after plating, showing the smaller size of organoids obtained from PrP KO mice. Bar, 200 μm. (C) E-cadherin, β-catenin, and KI-67 immunostaining of 7-d organoids. Although smaller and less abundant, PrP KO organoids have a normal epithelial organization, as shown by E-cadherin and β-catenin staining (top), but exhibit smaller, KI-67–positive crypt domains (bottom). Note that using the same focus for both genotypes, only part of the WT organoids may be visualized in the fields. Bar, 50 μm.

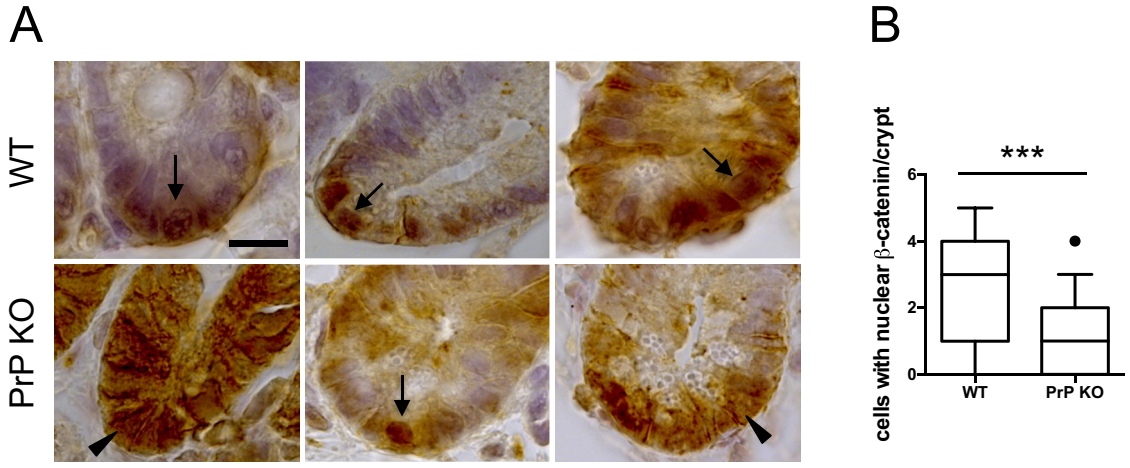

FIGURE 11: Altered nuclear β-catenin staining in the intestinal crypts of PrP-knockout mice. (A) Crypt sections of jejunum from WT and PrP-knockout mice were stained for β-catenin by immunohistochemistry. Arrows indicate examples of nuclear β-catenin, and arrowheads point out examples of diffuse and/or membranous staining. Bar, 10 μm. (B) Quantification of cells per crypt in which β-catenin was localized mainly in the nucleus. Thirty-four crypts from five WT mice and 55 crypts from five PrP-knockout mice were quantified. Whiskers mark the 10th and 90th percentiles, boxes mark the 25th and 75th percentiles, and the black circle represents an outlier. ***$p < 0.001$ (Student's *t* test).

Nuclei were pelleted by centrifugation at 1000 × *g* for 10 min at 4°C and washed in TKCM buffer, and nuclear proteins were extracted with 2 M NaCl in TKCM buffer for 1 h at 4°C. Excess NaCl was removed by overnight dialysis against phosphate-buffered saline (PBS) at 4°C. Nuclear proteins were immunoprecipitated with anti-PrP^c antibodies (Ab703; rabbit polyclonal antibody; Abcam, Cambridge, United Kingdom) and separated on 4–12% SDS/polyacrylamide gels. After staining with colloidal Coomassie blue (G250; Bio-Rad, Hercules, CA), the visualized bands were cut into 1-mm slices. Gel slices were then reduced, alkylated, and subjected to digestion with trypsin (Roche Diagnostics, Meylan, France). Extracted peptides were dried and solubilized in solvent A (95/5 water/acetonitrile in 0.1% [wt/vol] formic acid). The total digestion product of a gel slice was used per liquid chromatography–tandem mass spectrometry (MS/MS) analysis. The extracted peptides were concentrated and separated on an LC-Packing system (Dionex; Thermo Fisher Scientific, Illkirch, France) coupled to the nano-electrospray II ionization interface of a QSTAR Pulsar i (Applied Biosystems, Life Technologies, Saint Aubin, France) using a PicoTip (10-mm inner diameter; New Objectives, Woburn, MA). The MS/MS data were searched twice by using MASCOT (Matrix Science, London, United Kingdom) and PHENYX (Geneva Bioinformatics, Geneva, Switzerland) software on internal servers, first without taxonomic restriction to reveal the presence of proteins of interest and mammalian contaminants, then in the National Center for Biotechnology Information Human database (National Library of Medicine, Bethesda, MD). All data were manually verified in order to minimize errors in protein identification and/or characterization.

Immunofluorescence analyses and proximity ligation assay

Cells were seeded on glass coverslips (SW480 and HIEC-6 cells) or on Transwell filters (Caco-2/TC7 cells). After 2 or 8 d, cells were fixed with paraformaldehyde (4%, 30 min, room temperature) and permeabilized with Triton X-100 (0.1%, 30 min). Alternatively, for some antibodies, cells were fixed and permeabilized with methanol (5 min, –20°C). The following antibodies were used: anti-PrP^c (12F10, mouse monoclonal antibody, S.P.I. BIO, Montigny le Bretonneux, France; or Ab703, rabbit polyclonal antibody, Abcam), γ-catenin and β-catenin (mouse monoclonal antibodies; BD Biosciences, Erembodegem, Belgium), γ-catenin (rabbit polyclonal antibody; Abcam), E-cadherin (ECCD2, rat monoclonal antibody; TaKaRa Bio Europe, Saint-Germain-en-Laye, France), β-catenin and TCF7L2 (rabbit polyclonal antibodies; Cell Signaling, St Quentin en Yvelines, France), FLAG (mouse monoclonal antibody; Sigma-Aldrich, St Quentin-Fallavier, France), YAP1 (rabbit monoclonal antibody; WuXi AppTec, San Diego, CA), and KI-67 (rabbit polyclonal antibody; Abcam). Secondary antibodies were Alexa 488 and Alexa 546–conjugated anti–immunoglobulin G (IgG; Molecular Probes, St Aubin, France).

PLA was performed on cells processed as described for immunofluorescence, using two primary antibodies from mouse and rabbit and according to manufacturer's instructions (Olink Bioscience, Sigma-Aldrich). PLA PLUS and MINUS probes for mouse and rabbit and the Duolink Orange detection kit were used.

Nuclei were stained by 4′-6-diamidino-2-phenylindole (DAPI), and cells were examined by confocal microscopy (LSM 710 microscope; Carl Zeiss, Jena, Germany) using ZEN 2011 software. Quantifications were performed using a macro of ImageJ software (2.0.0; National Institutes of Health, Bethesda, MD).

Immunoprecipitation and Western blots

For total protein extraction, the cell layer was washed in cold PBS and scraped in TNE buffer (10 mM Tris, pH 8, 150 mM NaCl, 1 mM EDTA)/Nonidet P-40 (1%) supplemented with antiprotease and antiphosphatase cocktails (Sigma-Aldrich). Alternatively, nuclear/cytoplasmic protein fractions were purified using the Pierce NE-PER Nuclear and Cytoplasmic Extraction Reagents kit (Thermo Fisher Scientific, Illkirch, France) according to the manufacturer's instructions.

Protein concentrations were determined using the BC Assay (Uptima/Interchim, Montluçon, France).

Immunoprecipitations were performed on nuclear extracts with rabbit anti-PrP^c and anti–γ-catenin antibodies (Abcam) or nonimmune rabbit IgG (Sigma-Aldrich) as control coupled to protein

A–Sepharose CL 4B (Amersham Biosciences, GE Healthcare Europe, Orsay, France). For Western blots, samples were boiled for 10 min in Laemmli buffer and fractionated through 10 or 12% polyacrylamide gels under reducing conditions. The following antibodies were used: anti-PrP^c (mouse monoclonal SAF32; S.P.I. BIO), anti–γ-catenin and β-catenin (mouse monoclonal antibodies; BD Biosciences), and anti-TCF7L2 (rabbit polyclonal antibody; Cell Signaling). Anti-actin (Millipore), poly[ADP-ribose] polymerase 1 (PARP-1), specificity protein 1 (SP1), and lactate dehydrogenase (LDH; Santa Cruz Biotechnology, Santa Cruz CA) antibodies were used for cell fraction purity control. Bound antibodies were detected by chemiluminescence (ECL, Amersham Biosciences, GE Healthcare Europe; or ECL2 Pierce, Thermo Fisher Scientific) on a Luminescence Image Analyzer (LAS-4000; Fujifilm, Courbevoie, France). Densitometric semiquantitative analyses were performed using ImageJ software (2.0.0).

Site-directed mutagenesis, transfection experiments, and PLA quantifications

Mutagenesis was achieved by PCR using 50 ng of pFLAG-TCF7L2 (Idogawa *et al.*, 2005), the high-fidelity thermostable Phusion DNA polymerase (New England BioLabs, Evry, France) and the complementary mutagenic oligonucleotides listed in Supplemental Table S1. After PCR, the starting template was eliminated by *Dpn*I digestion, and the final products were used to transform competent bacteria from New England BioLabs. All selected mutants were sequenced before use.

SW480 cells were seeded on glass coverslips in 24-well plates (40,000 cells/well) and transfected 24 h later with the different Flag-TCF7L2 constructs (500 ng) using X-treme GENE HP DNA (Roche Diagnostics, Meylan, France) according to the manufacturer's instructions. PLA experiments were performed 2 d after transfection as described using mouse monoclonal anti-FLAG combined with rabbit anti-PrP^c, anti–β-catenin, or anti–γ-catenin antibodies. Expression of the different constructs was analyzed by immunofluorescence with the anti-FLAG antibody in parallel wells because PLA and immunofluorescent detection of FLAG tag could not be performed simultaneously owing to competition of PLA probes and secondary antibodies for fixation on primary anti-FLAG antibodies.

For confocal microscopy analysis, acquisition settings were chosen so that PLA signals for β-catenin/FLAG interactions, which gave the highest intensities, were close to the saturation level. The same settings were then kept constant for all interactions and all constructs, maximizing the dynamic range of quantification. Quantification of PLA signals for the different Flag-TCF7L2 constructs and for the different interactions was performed using a macro of ImageJ software (2.0.0). Integrated intensity of PLA signal normalized to cell number was measured in at least 10 random fields for each condition (total of ~1000 cells). After subtraction of background (mean intensity obtained for PLA assays with FLAG-empty vector), values were normalized to mean values of FLAG immunofluorescence signal/cell, to correct for variations in transfection efficiency.

Small interfering RNA transfection

siRNAs were purchased from Qiagen SA Biosciences (Courtaboeuf, France). Two different siRNA sequences were combined for each gene silencing (Supplemental Table S2). Cells were seeded at 20,000 cells/cm^2 on plastic or on glass coverslips and transfected 48 h after plating using X-tremeGENE siRNA Transfection Reagent (Roche Diagnostics). The total concentration of siRNA in the media was 200 nM.

TCF/β-catenin reporter assays

The TCF-responsive TOP-FLASH, expressing luciferase driven by multiple TCF-responsive elements, or FOP-FLASH with mutated TCF-responsive elements, were purchased from Millipore. The pRSV-β-gal encoding β-galactosidase was used as internal control. The vectors encoding human γ-catenin and mouse PrP^c were obtained from Eric Fearon (Addgene plasmid #16827; Caca *et al.*, 1999) and Susan Lindquist (Addgene plasmid #22109; Jackson *et al.*, 2009), respectively. The vector encoding a constitutively active mutant S33Y of β-catenin was obtained from Corinne Quittau-Prevostel (U1194, Institut de Recherche en Cancérologie, Montpellier, France).

COS7 or SW480 cells were plated into 12-well plates (120,000 and 80,000 cells/well, respectively). Transfection was performed 24 h after plating using X-tremeGENE HP DNA transfection reagent (Roche Diagnostics). Cells were transfected with 200 ng of TOP or FOP vector, together with 100 ng of pRSV-β-gal. COS7 received in addition 50 ng of S33Y β-catenin vector and either γ-catenin or PrP^c vector (100 or 300 ng). SW480 received only γ-catenin or PrP^c vector because β-catenin is constitutively stabilized in this cell line. The PTZ18R plasmid was used to adjust the quantity of plasmid DNA to 1 μg for all conditions. Cells were harvested 48 h after transfection, and β-galactosidase and luciferase activities were analyzed using a multifunctional microplate reader (FLUOSTAR Omega; BMG Labtech, Ortenberg, Germany).

TOP/FOP assays were also performed in SW480 after PrP^c silencing by siRNA. In this case, reporter plasmids and the mouse PrP^c expression vector were transfected 24 h after plating, and siRNAs were transfected the next day, as described. We showed previously that mouse PrP^c was not targeted by siRNA directed against the human mRNA (Petit *et al.*, 2012).

Purification of epithelial cells from mouse intestinal crypts

PrP^c-knockout mice, backcrossed on C57BL/6, and their wild-type counterparts were housed in pathogen-free conditions (Petit *et al.*, 2012). Ileum of 3-mo-old wild-type (five animals) or PrP^c-knockout mice (five animals) were collected, flushed with PBS containing 1 mM $CaCl_2$ and 0.5 mM $MgCl_2$, minced in 1-mm pieces, and transferred, as a pool, in a chelation buffer (27 mM trisodium citrate, 5 mM Na_2HPO_4, 96 mM NaCl, 8 mM KH_2PO_4, 1.5 mM KCl, 0.5 mM dithiothreitol, 55 mM D-sorbitol, 44 mM sucrose) at 4°C for shaking. According to the strength and number of agitations, five fractions of epithelial cells were obtained, corresponding to the villus tip (fraction 1) to the crypt bottom (fraction 5). Each cell fraction was centrifuged (1500 rpm, 5 min, 4°C); the cell pellet was resuspended in 800 μl of PBS^+ and stored at −80°C until RNA extraction. Analysis of the differential expression of a set of genes between the top and bottom fractions of the crypts and comparison with the results reported in Mariadason *et al.* (2005) confirmed the purity of the bottom crypt fraction.

RNA extraction and gene expression analyses

Total RNA was isolated from mouse epithelial crypt cells or cultured cell lines with Tri-Reagent (Molecular Research Center, Cincinnati, OH) according to manufacturer's instructions. After rDNase digestion (Macherey-Nagel, Hoerdt, France), RNA integrity was checked by gel electrophoresis. Reverse transcription (RT) was performed with 1 μg of RNA using Roche reagents (Roche Diagnostics). Real-time PCR was conducted with cDNA and both the sense and antisense oligonucleotides in a volume of 10 μl of SYBR green PCR mix (Agilent, Massy, France) and monitored and assessed in a Stratagene Mx3000P (Thermo Fisher Scientific) system. Values were

normalized to L19 or 18S for human cells or to cyclophilin expression for mouse cells. Primer sequences are given in Supplemental Table S3.

PCR array analysis

SW480 and HIEC-6 cells were transfected with siRNA 48 h after plating and collected 24 h after transfection for RNA extraction as described. After reverse transcription with the RT^2 First Strand Kit (Qiagen SA Biosciences) using 1 µg of RNA, silencing efficiency was checked by semiquantitative real-time PCR. A minimum of 80% extinction of the siRNA targets was a prerequisite to proceed further for PCR array analysis. Human WNT Signaling Targets RT^2 Profiler PCR Array Plate (Qiagen SA Biosciences), which profiles the expression of 84 target genes and eight control genes, was used with the RT^2 SYBR Green qPCR Mastermix and the Mx3000P Stratagene system. Genes were selected for heat map profiles when modulations of their expression, after normalization by manufacturer's controls, were ≥1.4× or ≤0.7× upon either PrP^c or γ-catenin silencing in at least one cell line, with similar values in three independent experiments and $p < 0.05$.

Immunohistochemistry on mouse intestinal crypts

For β-catenin staining in mouse crypts, wild-type and PrP-knockout mice were killed, and their intestines were removed, flushed gently with PBS, and fixed overnight at 4°C in alcohol/Formalin/acetic acid before being embedded in paraffin. Immunostaining with anti–β-catenin (rabbit polyclonal; Cell Signaling) was performed on 5-µm paraffin sections after antigen retrieval in boiling 10 mM citrate buffer (pH 6) for 10 min and permeabilization with 0.1% Triton X-100 (20 min). A horseradish peroxidase–labeled anti-rabbit antibody (Amersham Biosciences) and 3,3′-diaminobenzidine were used for revelation. β-Catenin staining was examined on a Zeiss Imager-M2 microscope using ZEN 2011 software.

Intestinal organoids

Isolation and culture of intestinal crypts were performed as previously described (Andersson-Rolf *et al*., 2014), with some modifications. Briefly, the small intestines of 4- to 5-mo-old wild-type or PrP-knockout mice were isolated, cut into 5-cm-long pieces, and washed in cleaning solution (PBS-C, phosphate-buffered saline, calcium/magnesium-free; 2% penicillin-streptomycin, 1% gentamicin; Life Technologies). Intestinal pieces were opened longitudinally, and villi were scraped off by using a coverslip. The tissue was washed by vigorous shaking in precooled PBS-C and transferred into a 1 mM EDTA solution in PBS-C for 30 min at 4°C on a rotating wheel. Villi were then removed by vigorous shaking (~20 times), and the tissue was incubated at 4°C for 1 h on a rotating wheel in Leibovitz medium (Sigma-Aldrich) supplemented with 5 mM EDTA, 2% penicillin-streptomycin, 1× GlutaMAX, and 25 mM HEPES (Life Technologies). To isolate the crypts, the tissue fragments were transferred into a precooled Leibovitz EDTA-free solution and vigorously shaken (~40 times). The presence of crypts was confirmed under the microscope and their number counted in a 30-µl drop of crypt solution. A volume containing 300 crypts was spun down at 300 × *g* for 5 min at 4°C, supernatant was discarded, and the pellet was resuspended in 150 µl of Matrigel (Corning) half-diluted in DMEM/F12 (Life Technologies). Crypts were then seeded into 48-well flat-bottom plates and incubated for 15 min at 37°C. Then, Matrigel was overlaid by 300 µl of ENR medium (DMEM/F12, 20 ng/ml EGF [Peprotech, Neuilly sur Seine, France], 10 ng/ml FGF [Peprotech], 100 ng/ml Noggin [Peprotech], 2.5% [vol/vol] GlutaMAX [Life Technologies], 500 ng/ml R-Spondin [R&D Systems, Lille, France], 1× B27 [Life Technologies], 1× N2 [Life Technologies]). The crypt number was evaluated after 6 d of culture by manual counting. Immunofluorescence staining was performed and analyzed as described after organoid fixation in 4% paraformaldehyde and permeabilization with Triton X-100 (0.3%, 10 min).

Statistical analysis

Values are expressed as mean ± SEM. Statistical analyses were performed using GraphPad Prism 6.0 (GraphPad Software, La Jolla, CA). The statistical significance of the differences between groups was determined by Student's *t* test, one-way or two-way analysis of variance (ANOVA), or nonparametric Mann–Whitney or Kruskal–Wallis test as appropriate. ANOVA and Kruskal–Wallis analyses were followed by Sidak or Tukey and Dunn multiple-comparison posttests, respectively. $p < 0.05$ was considered statistically significant.

ACKNOWLEDGMENTS

HIEC-6 cells were a generous gift from J. F. Beaulieu (University of Sherbrooke, Sherbrooke, Canada). We thank Magashi Idogawa (Sapporo Medical University, Sapporo, Japan) and Tesshi Yamada (National Cancer Center Research Institute, Tokyo, Japan) for the plasmid pFLAG-TCF4 (TCF7L2) and Corinne Quittau-Prevostel (Institut de Recherche en Cancérologie, Montpellier, France) for the plasmid encoding the S33Y mutant of β-catenin. We thank Ryad Boukherrouf for his participation in the study. Confocal microscopy was performed at the Centre d'Imagerie Cellulaire et de Cytométrie (Centre de Recherche des Cordeliers, UMRS 1138, Paris, France). Mice were housed in the SPF facility of the Centre de Recherche des Cordeliers. This work was supported by institutional funding from the Institut National de la Santé et de la Recherche Médicale, Université Pierre et Marie Curie and the Ecole Pratique des Hautes Etudes and a grant from the Agence Nationale pour la Recherche (ANR-09-JCJC-0052-01). L.S.B. was the recipient of a fellowship from the French Ministère de l'Enseignement Supérieur et de la Recherche.

REFERENCES

Aguilera O, Pena C, Garcia JM, Larriba MJ, Ordonez-Moran P, Navarro D, Barbachano A, Lopez de Silanes I, Ballestar E, Fraga MF, *et al.* (2007). The Wnt antagonist DICKKOPF-1 gene is induced by 1alpha,25-dihydroxyvitamin D3 associated to the differentiation of human colon cancer cells. Carcinogenesis 28, 1877–1884.

Aktary Z, Pasdar M (2012). Plakoglobin: role in tumorigenesis and metastasis. Int J Cell Biol 2012, 189521.

Andersson-Rolf A, Fink J, Mustata RC, Koo BK (2014). A video protocol of retroviral infection in primary intestinal organoid culture. J Vis Exp e51765.

Antony H, Wiegmans AP, Wei MQ, Chernoff YO, Khanna KK, Munn AL (2012). Potential roles for prions and protein-only inheritance in cancer. Cancer Metastasis Rev 31, 1–19.

Azzolin L, Zanconato F, Bresolin S, Forcato M, Basso G, Bicciato S, Cordenonsi M, Piccolo S (2012). Role of TAZ as mediator of Wnt signaling. Cell 151, 1443–1456.

Caca K, Kolligs FT, Ji X, Hayes M, Qian J, Yahanda A, Rimm DL, Costa J, Fearon ER (1999). Beta- and gamma-catenin mutations, but not E-cadherin inactivation, underlie T-cell factor/lymphoid enhancer factor transcriptional deregulation in gastric and pancreatic cancer. Cell Growth Differ 10, 369–376.

Chantret I, Rodolosse A, Barbat A, Dussaulx E, Brot-Laroche E, Zweibaum A, Rousset M (1994). Differential expression of sucrase-isomaltase in clones isolated from early and late passages of the cell line Caco-2: evidence for glucose-dependent negative regulation. J Cell Sci 107, 213–225.

Chen SN, Gurha P, Lombardi R, Ruggiero A, Willerson JT, Marian AJ (2014). The hippo pathway is activated and is a causal mechanism for adipogenesis in arrhythmogenic cardiomyopathy. Circ Res 114, 454–468.

Clevers H, Nusse R (2012). Wnt/beta-catenin signaling and disease. Cell 149, 1192–1205.
Crozet C, Vezilier J, Delfieu V, Nishimura T, Onodera T, Casanova D, Lehmann S, Beranger F (2006). The truncated 23–230 form of the prion protein localizes to the nuclei of inducible cell lines independently of its nuclear localization signals and is not cytotoxic. Mol Cell Neurosci 32, 315–323.
Guezguez A, Pare F, Benoit YD, Basora N, Beaulieu JF (2014). Modulation of stemness in a human normal intestinal epithelial crypt cell line by activation of the WNT signaling pathway. Exp Cell Res 322, 355–364.
Hatzis P, van der Flier LG, van Driel MA, Guryev V, Nielsen F, Denissov S, Nijman IJ, Koster J, Santo EE, Welboren W, *et al.* (2008). Genome-wide pattern of TCF7L2/TCF4 chromatin occupancy in colorectal cancer cells. Mol Cell Biol 28, 2732–2744.
Hosokawa T, Tsuchiya K, Sato I, Takeyama N, Ueda S, Tagawa Y, Kimura KM, Nakamura I, Wu G, Sakudo A, *et al.* (2008). A monoclonal antibody (1D12) defines novel distribution patterns of prion protein (PrP) as granules in nucleus. Biochem Biophys Res Commun 366, 657–663.
Idogawa M, Yamada T, Honda K, Sato S, Imai K, Hirohashi S (2005). Poly(ADP-ribose) polymerase-1 is a component of the oncogenic T-cell factor-4/beta-catenin complex. Gastroenterology 128, 1919–1936.
Jackson WS, Borkowski AW, Faas H, Steele AD, King OD, Watson N, Jasanoff A, Lindquist S (2009). Spontaneous generation of prion infectivity in fatal familial insomnia knockin mice. Neuron 63, 438–450.
Jaegly A, Mouthon F, Peyrin JM, Camugli B, Deslys JP, Dormont D (1998). Search for a nuclear localization signal in the prion protein. Mol Cell Neurosci 11, 127–133.
Liang J, Pan Y, Zhang D, Guo C, Shi Y, Wang J, Chen Y, Wang X, Liu J, Guo X, *et al.* (2007). Cellular prion protein promotes proliferation and G1/S transition of human gastric cancer cells SGC7901 and AGS. FASEB J 21, 2247–2256.
Linden R, Martins VR, Prado MA, Cammarota M, Izquierdo I, Brentani RR (2008). Physiology of the prion protein. Physiol Rev 88, 673–728.
Mange A, Crozet C, Lehmann S, Beranger F (2004). Scrapie-like prion protein is translocated to the nuclei of infected cells independently of proteasome inhibition and interacts with chromatin. J Cell Sci 117, 2411–2416.
Mariadason JM, Nicholas C, L'Italien KE, Zhuang M, Smartt HJ, Heerdt BG, Yang W, Corner GA, Wilson AJ, Klampfer L, *et al.* (2005). Gene expression profiling of intestinal epithelial cell maturation along the crypt-villus axis. Gastroenterology 128, 1081–1088.
Miravet S, Piedra J, Miro F, Itarte E, Garcia de Herreros A, Dunach M (2002). The transcriptional factor Tcf-4 contains different binding sites for beta-catenin and plakoglobin. J Biol Chem 277, 1884–1891.
Morel E, Fouquet S, Chateau D, Yvernault L, Frobert Y, Pincon-Raymond M, Chambaz J, Pillot T, Rousset M (2004). The cellular prion protein PrPc is expressed in human enterocytes in cell-cell junctional domains. J Biol Chem 279, 1499–1505.
Morel E, Fouquet S, Strup-Perrot C, Thievend CP, Petit C, Loew D, Faussat AM, Yvernault L, Pincon-Raymond M, Chambaz J, *et al.* (2008). The cellular prion protein PrP(c) is involved in the proliferation of epithelial cells and in the distribution of junction-associated proteins. PLoS One 3, e3000.
Moroishi T, Hansen CG, Guan KL (2015). The emerging roles of YAP and TAZ in cancer. Nat Rev Cancer 15, 73–79.
Mouillet-Richard S, Ermonval M, Chebassier C, Laplanche JL, Lehmann S, Launay JM, Kellermann O (2000). Signal transduction through prion protein. Science 289, 1925–1928.
Naslavsky N, Stein R, Yanai A, Friedlander G, Taraboulos A (1997). Characterization of detergent-insoluble complexes containing the cellular prion protein and its scrapie isoform. J Biol Chem 272, 6324–6331.
Petit CS, Barreau F, Besnier L, Gandille P, Riveau B, Chateau D, Roy M, Berrebi D, Svrcek M, Cardot P, *et al.* (2012). Requirement of cellular prion protein for intestinal barrier function and mislocalization in patients with inflammatory bowel disease. Gastroenterology 143, 122–132.e115.
Petit CS, Besnier L, Morel E, Rousset M, Thenet S (2013). Roles of the cellular prion protein in the regulation of cell adhesion, cell-cell junctions and barrier function. Tissue Barriers 1, e24377.
Pinto D, Gregorieff A, Begthel H, Clevers H (2003). Canonical Wnt signals are essential for homeostasis of the intestinal epithelium. Genes Dev 17, 1709–1713.
Prusiner SB (1998). Prions. Proc Natl Acad Sci USA 95, 13363–13383.
Rosenbluh J, Nijhawan D, Cox AG, Li X, Neal JT, Schafer EJ, Zack TI, Wang X, Tsherniak A, Schinzel AC, *et al.* (2012). beta-Catenin-driven cancers require a YAP1 transcriptional complex for survival and tumorigenesis. Cell 151, 1457–1473.
Rybner C, Finel-Szermanski S, Felin M, Sahraoui T, Rousseau C, Fournier JG, Seve AP, Botti J (2002). The cellular prion protein: a new partner of the lectin CBP70 in the nucleus of NB4 human promyelocytic leukemia cells. J Cell Biochem 84, 408–419.
Salomon D, Sacco PA, Roy SG, Simcha I, Johnson KR, Wheelock MJ, Ben-Ze'ev A (1997). Regulation of beta-catenin levels and localization by overexpression of plakoglobin and inhibition of the ubiquitin-proteasome system. J Cell Biol 139, 1325–1335.
Santuccione A, Sytnyk V, Leshchyns'ka I, Schachner M (2005). Prion protein recruits its neuronal receptor NCAM to lipid rafts to activate p59fyn and to enhance neurite outgrowth. J Cell Biol 169, 341–354.
Sato T, Vries RG, Snippert HJ, van de Wetering M, Barker N, Stange DE, van Es JH, Abo A, Kujala P, Peters PJ, *et al.* (2009). Single Lgr5 stem cells build crypt-villus structures in vitro without a mesenchymal niche. Nature 459, 262–265.
Shitashige M, Satow R, Honda K, Ono M, Hirohashi S, Yamada T (2008). Regulation of Wnt signaling by the nuclear pore complex. Gastroenterology 134, 1961–1971, 1971.e1–e4.
Stappenbeck TS, Wong MH, Saam JR, Mysorekar IU, Gordon JI (1998). Notes from some crypt watchers: regulation of renewal in the mouse intestinal epithelium. Curr Opin Cell Biol 10, 702–709.
Strom A, Wang GS, Picketts DJ, Reimer R, Stuke AW, Scott FW (2011). Cellular prion protein localizes to the nucleus of endocrine and neuronal cells and interacts with structural chromatin components. Eur J Cell Biol 90, 414–419.
van de Wetering M, Sancho E, Verweij C, de Lau W, Oving I, Hurlstone A, van der Horn K, Batlle E, Coudreuse D, Haramis AP, *et al.* (2002). The beta-catenin/TCF-4 complex imposes a crypt progenitor phenotype on colorectal cancer cells. Cell 111, 241–250.
Vey M, Pilkuhn S, Wille H, Nixon R, DeArmond SJ, Smart EJ, Anderson RG, Taraboulos A, Prusiner SB (1996). Subcellular colocalization of the cellular and scrapie prion proteins in caveolae-like membranous domains. Proc Natl Acad Sci USA 93, 14945–14949.
Westergard L, Christensen HM, Harris DA (2007). The cellular prion protein (PrP(C)): its physiological function and role in disease. Biochim Biophys Acta 1772, 629–644.
Yan Y, Lackner MR (2012). FOXO3a and beta-catenin co-localization: double trouble in colon cancer? Nat Med 18, 854–856.
Zhao B, Ye X, Yu J, Li L, Li W, Li S, Yu J, Lin JD, Wang CY, Chinnaiyan AM, *et al.* (2008). TEAD mediates YAP-dependent gene induction and growth control. Genes Dev 22, 1962–1971.
Zhurinsky J, Shtutman M, Ben-Ze'ev A (2000). Differential mechanisms of LEF/TCF family-dependent transcriptional activation by beta-catenin and plakoglobin. Mol Cell Biol 20, 4238–4252.